



ELSEVIER

Available online at [www.sciencedirect.com](http://www.sciencedirect.com)

SCIENCE @ DIRECT®

International Journal of Plasticity 22 (2006) 654–684

INTERNATIONAL JOURNAL OF  
**Plasticity**

[www.elsevier.com/locate/ijplas](http://www.elsevier.com/locate/ijplas)

# A physically based gradient plasticity theory

Rashid K. Abu Al-Rub, George Z. Voyiadjis \*

*Department of Civil and Environmental Engineering, Louisiana State University,  
CEBA 3508-B, Baton Rouge, LA 70803, USA*

Received 15 January 2004  
Available online 28 July 2005

---

## Abstract

The intent of this work is to derive a physically motivated mathematical form for the gradient plasticity that can be used to interpret the size effects observed experimentally. The step of translating from the dislocation-based mechanics to a continuum formulation is explored. This paper addresses a possible, yet simple, link between the Taylor's model of dislocation hardening and the strain gradient plasticity. Evolution equations for the densities of statistically stored dislocations and geometrically necessary dislocations are used to establish this linkage. The dislocation processes of generation, motion, immobilization, recovery, and annihilation are considered in which the geometric obstacles contribute to the storage of statistical dislocations. As a result, a physically sound relation for the material length scale parameter is obtained as a function of the course of plastic deformation, grain size, and a set of macroscopic and microscopic physical parameters. Comparisons are made of this theory with experiments on micro-torsion, micro-bending, and micro-indentation size effects.

© 2005 Elsevier Ltd. All rights reserved.

*Keywords:* Gradient plasticity; Material length scale; SSDs; GNDs; Size effects; Micro-bending; Micro-torsion; Micro-indentation

---

---

\* Corresponding author. Tel.: +1 225 578 8668; fax: +1 225 578 9176.

*E-mail addresses:* [rabuall@lsu.edu](mailto:rabuall@lsu.edu) (R.K. Abu Al-Rub), [Voyiadjis@eng.lsu.edu](mailto:Voyiadjis@eng.lsu.edu) (G.Z. Voyiadjis).

## 1. Introduction

The problem in developing a macroscopic model embedded with a micromechanical-based theory of inelasticity which could be used as an engineering theory for both the analysis and in computer-aided design of materials is a topical and still unsolved material science problem. Attempts to construct such a theory are faced with the difficulties in describing the microscopic structure of materials in terms of macroscopic mechanics. On the other hand, at the present time, it is still not possible to perform quantum and atomistic simulations on realistic time scale and structures. When load is applied, the inelastic deformation that occurs in most cases is not homogeneous, but reveals fluctuations on various length scales. This heterogeneity plays a key role in determining the macroscopic properties of materials. A physically based theory that bridges the gap between the conventional continuum theories and the micromechanical theories should be developed as a remedy for this situation.

Material length scales (i.e., the dependence of mechanical response on the structure size) are of great importance to many engineering applications. Moreover, the emerging areas of micro and nanotechnologies exhibit important strength differences that result from continuous modification of the material microstructural characteristics with changing size, whereby the smaller is the size the stronger is the response. There are many experimental observations which indicate that, under certain specific conditions, the specimen size may significantly affect deformation and failure of the engineering materials and a length scale is required for their interpretation. Experimental work on particle-reinforced composites has revealed that a substantial increase in the macroscopic flow stress can be achieved by decreasing the particle size while keeping the volume fraction constant (Lloyd, 1994; Rhee et al., 1994; Zhu and Zbib, 1995; Nan and Clarke, 1996; Kiser et al., 1996). A similar strengthening effect associated with decreasing the diameter of thin wires in micro-torsion test has been reported by Fleck et al. (1994) and with decreasing the thickness of thin beams in micro-bending test has been reported by Stolken and Evans (1998), Shrotriya et al. (2003), and Haque and Saif (2003). Moreover, micro- and nano-indentation tests have shown that the material hardness increases with decreasing indentation size (e.g., Stelmashenko et al., 1993; DeGuzman et al., 1993; Ma and Clarke, 1995; Poole et al., 1996; McElhaney et al., 1998; Lim and Chaudhri, 1999; Elmustafa and Stone, 2002; Swadener et al., 2002). Indentation of thin films shows an increase in the yield stress with decreasing the film thickness (Huber et al., 2002). An experimental work by Taylor et al. (2002) shows an increase in the flow stress with decreasing hole size for geometrically similar perforated plates under tension, i.e., plates with a hole or several holes. Furthermore, there are many other well-known problems that show strong size effects. One example is the testing of polycrystalline materials which shows an increase in both yield and flow stresses, or equivalently the hardness, with decreasing the grain diameter; the so-called Hall-Petch behavior. These experiments have, thus, shown increasing in strength with decreasing size at the micron and submicron scales where the representative length scale  $\ell$  of the deformation field sets the qualitative and quantitative behavior of the size effect.

The aforementioned dependence of mechanical response on size could not be explained by the classical continuum mechanics since no length scale enters the constitutive description. A multiscale continuum theory, therefore, is needed to bridge the gap between the classical continuum theories and micromechanical theories. In all of the problems mentioned above, a continuum approach is appropriate since the collective nature of material defects is sufficiently large and faraway from individuality. Since the increase in strength with decreasing scale can be related to proportional increase in the strain gradients in each of the aforementioned experiments, the gradient plasticity theory has been successful in addressing the size effect problem. This success stems out from the incorporation of a microstructural length scale parameter through functional dependencies on the plastic strain gradient of nonlocal media (Aifantis, 1984, 1987). The gradient-dependent theory abandons the assumption that the stress at a given point is uniquely determined by the history of strain at this point only. It takes into account possible interactions with other material points in the vicinity of that point. However, in the past decade, the physical basis of the gradient plasticity theory for metals has been founded on theoretical developments concerning geometrically necessary dislocations (GNDs). Standard micromechanical modeling of the inelastic material behavior of metallic single crystals and polycrystals is commonly based on the premise that resistance to glide is due mainly to the random trapping of mobile dislocations during locally homogeneous deformation. Such trapped dislocations are commonly referred to as statistically stored dislocations (SSDs), and act as obstacles to further dislocation motion, resulting in hardening. As anticipated in the work of Ashby (1970), an additional contribution to the density of immobile dislocations and so to hardening can arise when the continuum length scale approaches that of the dominant microstructural features (e.g., mean spacing between inclusions relative to the inclusion size when considering a microstructure with dispersed inclusions, size of the plastic process zone at the front of the crack tip, the mean spacing between dislocations, the grain size, etc.). Indeed, in this case, the resulting deformation incompatibility between, e.g., “hard” inclusions and a “soft” matrix, is accommodated by the development of GNDs. An extensive review of the recent developments in gradient-dependent theory can be found in Voyiadjis et al. (2003, 2004) and Abu Al-Rub and Voyiadjis (2004a,b). A short review of these developments is presented here.

Many researchers have contributed substantially to the gradient approach with emphasis on numerical aspects of the theory and its implementation in finite element codes: Lasry and Belytschko (1988), Zbib and Aifantis (1988); and de Borst and co-workers (e.g., de Borst and Mühlhaus, 1992; de Borst et al., 1993; Pamin, 1994; de Borst and Pamin, 1996). Gradient thermodynamic plasticity and damage models were also introduced by Fremond and Nedjar (1996), Valanis (1996), and Voyiadjis et al. (2001, 2003, 2004). In parallel, other approaches that have length scale parameters in their constitutive structure (commonly referred to as nonlocal integral theories) have appeared as an outgrowth of earlier work by Eringen in nonlocal continuum elasticity and phenomenological hardening plasticity (e.g., Eringen and Edelen, 1972) and Bazant in strain softening media (e.g., Pijaudier-Cabot and Bazant, 1987; Bazant and Pijaudier-Cobot, 1988). Another class of gradient theories

have advocated in the last decade that assume higher-order gradients of the displacement field (e.g., Fleck et al., 1994; Fleck and Hutchinson, 1993, 1997, 2001; Nix and Gao, 1998; Gao et al., 1999a,b; Huang et al., 2000a; Gao and Huang, 2001; Hwang et al., 2002; Gurtin, 2002, 2003). This group of theories is in fact a particular case of generalized continua, such as *micromorphic continua* (Eringen, 1968), or *continua with microstructure* (Mindlin, 1964), which were all inspired by the pioneering work of the Cosserat brothers (Cosserat and Cosserat, 1909). The *Cosserat continuum* (or *micropolar continuum*) enhances the kinematic description of deformation by an additional field of local rotations, which can depend on the rotations corresponding to the displacement field, i.e., on the skew-symmetric part of the displacement gradient for the small displacement theory, or on the rotational part of the polar decomposition in the large-displacement theory. However, the works of Mindlin, Cosserat, and Eringen are based on the classical balances of linear and angular momentum. In contrast, the works of Fleck and Gurtin involve the introduction of additional balances over and above these classical balances; e.g., for single-crystal plasticity there is a new balance for each slip system involving forces that expend power in consort with slip on that system. In this connection, a similarly motivated strain gradient theory of plasticity based on incompatible lattice deformations is advanced by Acharya and Bassani (2000) and Bassani (2001). However, this theory preserves the same structure of classical plasticity. All the aforementioned theories include in their structure explicit material length scale measures. Incorporation of rate-dependent viscous terms introduces an implicit length scale measure and limits localization in dynamic or quasi-static problems (e.g., Perzyna, 1963; Needleman, 1988; Wang et al., 1998). However, the use of viscoelastic theories for scale-dependent problems is questionable and very limited work has been done in that direction (Voyiadjis et al., 2003, 2004).

The gradient theory has been applied to interpret size-dependent phenomena including, shear banding, micro- and nano-indentation, twist of thin wires, bending of thin films, void growth, crack tip plasticity, fine-grained metals, strengthening in metal matrix composites, multilayers, etc. (see Qiu et al., 2003 for a detailed review). Therefore, practical applications of gradient-dependent theories include, but not limited to, sensors, actuators, microelectromechanical systems (MEMS), microelectronic packaging, advanced composites, micromachining, welds, and functionally graded materials. However, the full utility of the gradient-type theories in bridging the gap between modeling, simulation, and design of modern technology hinges on one's ability to determine accurate values for the constitutive length scale parameter that scales the effects of strain gradients. The study of Begley and Hutchinson (1998), Shu and Fleck (1998), and Abu Al-Rub and Voyiadjis (2004a,b) indicated that indentation experiments might be the most effective test for measuring the length scale parameter  $\ell$ . Nix and Gao (1998) estimated the material length scale parameter  $\ell$  from the micro-indentation experiments of McElhaney et al. (1998) to be  $\ell = 12 \mu\text{m}$  for annealed single crystal copper and  $\ell = 5.84 \mu\text{m}$  for cold worked polycrystalline copper. Yuan and Chen (2001) proposed that the unique intrinsic material length parameter  $\ell$  can be computationally determined by fitting the Nix and Gao (1998) model from micro-indentation experiments and they have identified

$\ell$  to be 6  $\mu\text{m}$  for polycrystal copper and 20  $\mu\text{m}$  for single crystal copper. By fitting micro-indentation hardness data, [Begley and Hutchinson \(1998\)](#) have estimated that the length scale associated with the stretch gradients ranges from 1/4 to 1  $\mu\text{m}$ , while the material lengths associated with rotation gradients are on the order of 4  $\mu\text{m}$ . Other tests also have been used to determine  $\ell$ . Based on [Fleck et al. \(1994\)](#) micro-torsion tests of thin copper wires and [Stolken and Evans \(1998\)](#) micro-bend tests of thin nickel beams, the material length parameter is estimated to be  $\ell = 4 \mu\text{m}$  for copper and  $\ell = 5 \mu\text{m}$  for nickel. Recently, [Abu Al-Rub and Voyiadjis \(2004a,b\)](#) and [Voyiadjis and Abu Al-Rub \(2004\)](#) proposed a dislocation mechanics-based analytical model of a solid being indented with a spherical or pyramidal indenters to obtain values for the length scale parameter. The values of  $\ell$  inferred from micro and nano-hardness results for a number of materials lies within the range of 1/4 to 5  $\mu\text{m}$ , with the hardest materials having the smallest values of  $\ell$ .

Moreover, in spite of the crucial importance of the length scale parameter in gradient theory, very limited work is focused on the physical origin of this length scale parameter. The discrete dislocation origin of this length scale is rarely clear and its value is a free parameter. Phenomenological expressions have been assumed for the length scale parameter in gradient theory by [Aifantis and co-workers \(Konstantinidis and Aifantis, 2002; Tsagrakis and Aifantis, 2002\)](#). However, initial attempts have been made to relate  $\ell$  to the microstructure of the material. [Nix and Gao \(1998\)](#) identified  $\ell$  as  $L^2/b$ , where  $L$  is the average spacing between dislocation and  $b$  is the magnitude of the Burgers vector. Moreover, [Abu Al-Rub and Voyiadjis \(2004a,b\)](#) and [Voyiadjis and Abu Al-Rub \(2005\)](#) found  $\ell$  to be proportional to the mean path of the dislocation ( $L$ ). [Abu Al-Rub and Voyiadjis \(2004b\)](#) also derived an evolution equation for  $\ell$  as a function of temperature, strain, strain rate, and a set of measurable microstructural physical parameters.

However, it is questionable whether a unique value of the internal length scale can describe the size effect for different problems. There are indications that a fixed value of the material length scale is not always realistic and that different problems could require different values. [Aifantis and co-workers \(e.g., Aifantis, 1999; Tsagrakis and Aifantis, 2002; Zaiser and Aifantis, 2003; Zbib and Aifantis, 2003\)](#) have used different values of the length scale parameter for copper material to fit the [Fleck et al. \(1994\)](#) micro-torsion test results and different values for nickel to fit [Stolken and Evans \(1998\)](#) micro-bending test results. [Haque and Saif \(2003\)](#) showed that the length scale parameter is not fixed and depends on the grain size. Moreover, the findings of [Abu Al-Rub and Voyiadjis \(2004a,b\)](#), [Voyiadjis and Abu Al-Rub \(2005\)](#), and [Nix and Gao \(1998\)](#) that the material length scale is proportional with the mean free path indicate that  $\ell$  is not a fixed material parameter but changes with the deformation of the microstructure because of the variation of the mean free path with dislocation evolution. The change in the magnitude of  $\ell$  is also physically sound since the continuous modification of material characteristics with deformation. [Abu Al-Rub and Voyiadjis \(2004a\)](#) showed a dependence of  $\ell$  on the plastic strain level, as well as on the hardening level. Moreover, [Voyiadjis and Abu Al-Rub \(2005\)](#) found that the length scale varies with the course of plastic deformation, grain size, characteristic dimension of the

specimen, and hardening exponent. Some authors also argued the necessity of a length scale parameter in the gradient theories that change with plastic strain in order to achieve an efficient computational convergence while conducting multi-scale simulations (e.g., Pamin, 1994; de Borst and Pamin, 1996; Yuan and Chen, 2001).

In this work, the step of translating from the dislocation-based mechanics to a continuum formulation is explored. The mechanism-based strain gradient (MSG) plasticity theory (e.g., Nix and Gao, 1998; Gao et al., 1999a; Huang et al., 2000a, 2004; Hwang et al., 2002, 2003; Qiu et al., 2003) and the Taylor-based non-local theory (TNT) of plasticity (Gao and Huang, 2001; Guo et al., 2001) have been founded on the Taylor-type flow stress as their starting point. However, SSD density has not been treated explicitly in the aforementioned theories; instead, their effects on mechanical behavior have been described by strength evolution equations. In other words, if the flow stress, in the absence of strain gradients, depends on the plastic strain  $\varepsilon^p$  it follows that the density of SSDs is proportional to  $(\varepsilon^p)^2$ . Then, strain gradients are incorporated into the higher-order theory by taking the flow stress dependence to be  $((\varepsilon^p)^2 + \ell \partial \varepsilon^p / \partial x)^{1/2}$ . This choice is tantamount to assuming that the GNDs have no direct influence on the accumulation of the SSDs. In this paper, we introduce a gradient plasticity theory for metals that is based on strong basis of crystallographic dislocation mechanics. This theory is based on the Taylor's dislocation hardening model and assumes a simple addition of the densities from SSDs and GNDs. Based on the approaches of Kocks (1966, 1976), Estrin and Mecking (1984), Kubin and Estrin (1990), Bammann (2001), and Beaudoin and Acharya (2001), evolution equation for the densities of SSDs and GNDs are utilized to establish the bridge between dislocation-based theories and gradient continuum theories. The dislocation processes of generation, motion, immobilization, recovery, and annihilation are considered in which the GNDs contribute to the storage of SSDs. Moreover, a physically based expression for the length scale parameter as a function of effective plastic strain, grain size, and a set of macroscopic and microscopic parameters is derived. We use the proposed model to investigate the micro-bending of thin beams, micro-torsion of thin wires, and indentation size effect. We also show that the proposed gradient plasticity theory provides accurate predictions when compared to the experimental results of Stolken and Evans (1998) for micro-bending of annealed nickel thin films, of Shrotriya et al. (2003) for micro-bending of LIGA nickel thin films, of Haque and Saif (2003) for micro-bending of aluminum thin films, of Fleck et al. (1994) for micro-torsion of copper thin wires, of McElhaney et al. (1998) for micro-indentation of cold-worked copper, and of Poole et al. (1996) for micro-indentation of annealed polycrystalline copper.

The layout of this paper is as follows: In Section 2, the physical and micromechanical bases of the proposed gradient plasticity are presented. In Sections 3, the formulation and the constitutive relations of the proposed gradient plasticity theory are presented. Finally, in Section 4 we use the proposed gradient plasticity theory to investigate the size effect phenomena encountered in micro-bending of thin films, micro-torsion of thin wires, and micro-indentation.

## 2. Crystallographic dislocation density basis

From a microscopic point of view, plastic deformation in metallic materials reflects the collective behavior of a vast number of dislocations. Therefore, crystallographic dislocation densities, which are defined by their magnitude  $\rho$  measured in line length per unit volume, are suitable measures of plastic deformation in metals. The plastic strain is directly related to the motion of dislocations and the hardening of metals is attributed to the interaction of dislocations with each other and with surrounding crystal microstructure. The driving force behind these phenomena is the dislocation multiplication mechanisms: cross-slip and double cross-slip, glide, climb, etc. Moreover, dislocations can form loops, pile up on the grain boundaries and precipitate particles, and arrange themselves in various types of cells or substructures called dislocation networks. These arrangements act as obstacles to the motion of other dislocations, thus, providing the important mechanism of hardening. Therefore, what determines the hardening of the material is the ease with which dislocations are able to move and the simplest dislocation model should distinguish at least two types of dislocations: mobile and immobile. Motion of mobile dislocations carries the plastic strain, and immobile dislocations contribute to the plastic hardening. With an increase in the immobile dislocations, the mobile dislocations begin to have more interactions with the immobile dislocations such that movement becomes more difficult and the stress required to produce additional plastic strain increases, i.e., the material hardens.

The direct simulation of the dislocation processes, for example by using the discrete dislocation dynamics, is costly and, hence, the average treatment of dislocation processes is favorable and the concept of dislocation density is found useful. The dislocation density concept links the macroscopic stresses and strain to the underlying microstructural processes of plastic deformation and can be incorporated into the continuum theories to bridge the length scales.

The critical shear stress that is required to untangle the interactive dislocations and to induce a significant plastic deformation is defined as the Taylor flow stress,  $\tau$  (Taylor, 1938). The Taylor flow stress can also be viewed as the passing stress for a moving dislocation to glide through a forest of immobile dislocations without being pinned. The Taylor hardening law, which relates the shear strength to the dislocation density, has been the basis of the mechanism-based strain gradient (MSG) plasticity theory (e.g., Nix and Gao, 1998; Gao et al., 1999a; Huang et al., 2000a; Hwang et al., 2002; Qiu et al., 2003; Hwang et al., 2003; Huang et al., 2004) and the Taylor-based nonlocal theory (TNT) of plasticity (Gao and Huang, 2001; Guo et al., 2001). It gives a simple description of the dislocation interaction processes at the microscale (i.e., over a scale which extends from about a fraction of a micron to tens of microns). A generally accepted form for the Taylor's hardening law is

$$\tau = \tau_0 + \alpha Gb\sqrt{\rho_i}, \quad (1)$$

where  $\rho_i$  is the immobile or forest dislocation density,  $G$  is the shear modulus,  $b$  is the magnitude of the Burgers vector, and  $\alpha$  is a material constant related to the crystal and grain structure and usually ranging from 0.1 to 0.5 (Ashby, 1970).

The stress  $\tau_0$  is the extrapolated stress to zero dislocation density (strain independent *friction stress*).

Generally, it is assumed that the immobile or forest dislocation density,  $\rho_i$ , represents the total coupling between two types of dislocations which play a significant role in the hardening mechanism. Material deformation in metals enhances the dislocation formation, the dislocation motion, and the dislocation storage. The dislocation storage causes material hardening. The stored dislocations generated by trapping each other in a random way are referred to as statistically stored dislocations (SSDs), while the stored dislocations that maintain the plastic deformation compatibilities (continuity) within the polycrystal (or various components of the material) caused by nonuniform dislocation slip are called geometrically necessary dislocations (GNDs). Their presence causes additional storage of defects and increases the deformation resistance by acting as obstacles to the SSDs (Ashby, 1970). Therefore, as far as the experimental findings up to date, one cannot assume that GNDs are similar to the SSDs since both are different in nature and both contribute to the hardening and thus to the shear flow stress  $\tau$  given by Eq. (1). SSD density is dependent on the plastic strain,  $\varepsilon^p$ , while GND density is dependent on the plastic strain gradient,  $\partial\varepsilon^p/\partial x$  (Ashby, 1970; Fleck and Hutchinson, 1997; Arsenlis and Parks, 1999). In a continuum theory, these two contributions can be combined in various ways for which there is little guidance from dislocation mechanics (Fleck et al., 1994; Hutchinson, 2000). Abu Al-Rub and Voyiadjis (2004a,b) and Voyiadjis and Abu Al-Rub (2005) assumed that the forest dislocation density increases in proportion to the measure  $((\varepsilon^p)^{\gamma_1} + (\ell\partial\varepsilon^p/\partial x)^{\gamma_2})^{1/\gamma_3}$ , where  $\gamma_1$ ,  $\gamma_2$ , and  $\gamma_3$  are assumed as phenomenological material constants, termed there as *interaction coefficients*. These coefficients are introduced in order to assess the sensitivity of the predictions to the way in which the SSDs and GNDs are coupled. The couple stress theory of Fleck et al. (1994) assumes that  $\gamma_1 = \gamma_2 = \gamma_3 = 2$  based on mathematical reasons and not physical ones. The work of Aifantis and his co-workers (e.g., Aifantis, 1984, 1987; Zbib and Aifantis, 1988; Mühlhaus and Aifantis, 1991; Aifantis, 1999; Tsagrakis and Aifantis, 2002; Zaiser and Aifantis, 2003; Zbib and Aifantis, 2003) falls within the definition of  $\gamma_1 = \gamma_2 = \gamma_3 = 1$ . The MSG and TNT plasticity theories assume  $\gamma_1 = \gamma_3 = 2$ ,  $\gamma_2 = 1$ .

As the simplest possible relationship for the density of immobile (forest) dislocations is the direct sum of the densities of SSDs and GNDs. This was the basic assumption in formulating the couple stress gradient theory, the mechanism-based strain gradient plasticity theory, and the Taylor-based nonlocal theory of plasticity, such that Eq. (1) is written as

$$\tau = \tau_0 + \alpha Gb \sqrt{\rho_S + \rho_G}, \quad (2)$$

where  $\rho_S$  is the density of SSDs and  $\rho_G$  is the density of GNDs.

The macroscopic shear stress  $\tau$  is related to the corresponding tensile flow stress via the Taylor factor  $m$  as follows:

$$\sigma = \sigma_0 + m\alpha Gb \sqrt{\rho_S + \rho_G}, \quad (3)$$

where  $\sigma_0 = m\tau_0$  is the initial yield stress. The Taylor factor  $m$  acts as an isotropic interpretation of the crystalline anisotropy at the continuum level;  $m = \sqrt{3}$  for an

isotropic solid and  $m = 3.08$  for FCC polycrystalline metals (Taylor, 1938; Kocks, 1976). Eq. (2) constitutes the nonlocal micromechanical plasticity due to the presence of GNDs.

The validity of the Taylor relationship has been verified by numerous theoretical and experimental studies on metals and alloys (see, e.g., Hirsch, 1975) and, therefore, one may indeed use Eq. (1) as a starting point. However, Mughrabi (2001) concluded that, in the Taylor-type descriptions of the macroscopic flow stress, the simple superposition of the density of GNDs on the density of SSDs is *not well founded* and they are unambiguously related. Abu Al-Rub and Voyiadjis (2004a,b) and Voyiadjis and Abu Al-Rub (2005) presented different forms of Eq. (2) that enhance nonlinear couplings between  $\rho_S$  and  $\rho_G$  and they introduced three different interaction coefficients in order to assess the sensitivity of predictions to the way in which the coupling between the SSDs and GNDs is enhanced during the plastic deformation process. Furthermore, they showed that by incorporating these interaction coefficients in the gradient plasticity theory a suitable remedy is given to the Nix and Gao (1998) and Swadener et al. (2002) indentation size effect models in predicting the hardness values from micro/nano-indentation tests.

Moreover, in spite of the considerable progress made in recent years in the field of discrete dislocation modeling (see, e.g., Zbib et al., 1998), a detailed and realistic description of the evolution of the distributions and interactions among large number of SSDs and GNDs of different strengths does not seem feasible at the present time. Therefore, a more sophisticated description for the interaction between SSDs and GNDs would have to be explored (Arsenlis et al., 2004). In view of the complexity of this problem, the objectives of the present work, which is complementary to a parallel publication (Abu Al-Rub and Voyiadjis, 2004a,b; Voyiadjis and Abu Al-Rub, 2005) will be much more modest. In the present study, the problem outlined above will be treated at a very simple level in terms of a physical continuum formulation incorporating the evolutions of SSD and GND densities in order to accurately describe the plasticity of the polycrystal at micron and sub-micron length scales. Thus, it is necessary to have a model for strain hardening of a material that considers dislocation generation, motion, immobilization, recovery, and annihilation. Moreover, it is necessary to have a model for strain hardening of a material that considers the strain path dependence. All these physical features were not incorporated in the derivation of the couple stress gradient theory of Fleck and co-workers, and in the mechanism-based strain gradient (MSG) plasticity theory and the Taylor-based non-local plasticity theory (TNT) of Gao and co-workers. Most commonly a kind of evolution equation is derived for each type of dislocation density, which may generally be expressed in the form of hardening term-recovery term

$$\dot{\rho} = \dot{\rho}^{(+)} - \dot{\rho}^{(-)}, \quad (4)$$

where the superscripts (+) and (–) designate generation and recovery, respectively.

The evolution equation for the GND density,  $\dot{\rho}_G$ , is easier to develop than that for the SSD density,  $\dot{\rho}_S$ , because it is closely connected to the nonhomogeneous nature of plastic deformation. The GND density is related to the incompatibility of the plastic deformation and to the curvature of the crystal lattice. In fact, it is that portion of

the total density specifically needed to maintain the continuity of the crystal lattice (Arsenlis and Parks, 1999; Arsenlis et al., 2004). However, GND density cannot be spontaneously created or annihilated in a volume, as can SSD density. Instead, GND density must be transported to/from other regions, or result from local geometric reactions of existing GNDs (Arsenlis et al., 2004). If one considers a material element subjected to an increment of effective (shear) plastic strain  $\dot{\gamma}^p$  and its gradient  $\partial\dot{\gamma}^p/\partial x$  with associated increments of dislocation densities  $\dot{\rho}_S$  and  $\dot{\rho}_G$ , then GNDs accumulate in proportion to the strain gradient such that  $\dot{\rho}_G$  can be expressed as (e.g., Ashby, 1970; Nix and Gao, 1998; Arsenlis and Parks, 1999; Gao et al., 1999a,b, Huang et al., 2000a; Hutchinson, 2000; Svendsen, 2002)

$$\dot{\rho}_G = \frac{\bar{r}}{b} \frac{\partial\dot{\gamma}^p}{\partial x}, \tag{5}$$

where  $\bar{r}$  is the Nye factor introduced by Arsenlis and Parks (1999) to reflect the scalar measure of GND density resultant from macroscopic plastic strain gradients. For FCC polycrystals, Arsenlis and Parks (1999) have reported that the Nye factor has a value of  $\bar{r} = 1.85$  in bending and a value of  $\bar{r} = 1.93$  in torsion.

Next we will consider the evolution of the SSD density,  $\dot{\rho}_S$ , which has not been treated explicitly in MSG and TNT plasticity theories; instead, their effects on mechanical behavior have been described by strength evolution equations. In other words, if the flow stress, in the absence of strain gradients, depends on the plastic strain  $\varepsilon^p$ , then it follows that the density of SSDs is proportional to  $(\varepsilon^p)^2$ . Consequently, the strain gradients are incorporated into the higher-order theory by taking the flow stress dependence to be  $((\varepsilon^p)^2 + \ell\partial\varepsilon^p/\partial x)^{1/2}$ . This choice is tantamount to assuming that the GNDs have no direct influence on the accumulation of the SSDs. However, in this work, the evolution of the SSD density,  $\dot{\rho}_S$ , is the cumulative result of their multiplication, mutual annihilation and trapping, and their immobilization through interaction with other immobile dislocations (such as GNDs).

In fact, material hardening due to SSD accumulation is often described by means of the so-called Kocks’ model (e.g., Kocks, 1966, 1976; Estrin and Mecking, 1984; Kubin and Estrin, 1990) with limited geometric information:

$$\dot{\rho}_S = \left( \frac{k_1}{b} \sqrt{\rho_S} - k_2 \rho_S \right) \dot{\gamma}^p, \tag{6}$$

where  $k_1$  and  $k_2$  are functions to be determined later from basic dislocation principles. In the right hand side of Eq. (6), the dislocation storage/multiplication term  $k_1\sqrt{\rho_S}$  represents the combined rate at which mobile dislocations are immobilized and annihilated, while the term  $k_2\rho_S$  represents dynamic recovery which measures the probability by which immobile dislocations remobilize. Moreover, Eq. (6) shows that the rate of SSDs,  $\dot{\rho}_S$ , depends on the strain rate, which means that dislocations are less mobile when the material hardens. Therefore, one can assume that the mobile dislocation density is much smaller than the immobile dislocation density and it is strain independent (Bergstrom and Hallen, 1982).

During plastic deformation, the density of SSDs increases due to a wide range of processes that lead to production of new dislocations. Those new generated

dislocations travel on a background of GNDs which act as obstacles to the SSDs. Therefore, it is imperative to note that Eq. (6) does not take into account the effect of GNDs, and thus cannot allow the incorporation of higher-order gradients. Other authors (e.g., [Bammann and Aifantis, 1982](#); [Sluys and Estrin, 2000](#)) model the SSDs accumulation due to dislocation interaction and annihilation by means of a reaction–diffusion system. In this approach, the dependence of the evolution of SSD density on gradients of density is postulated and evolution equations for mobile dislocation density and immobile (forest) dislocation density are also developed. However, the evolution of GNDs is not explicitly considered in these models.

Therefore, in order to complement the evolution of the SSD density, Eq. (6) must be extended to include explicitly the effect of GNDs. This will allow us to combine the evolution equations for the SSD and GND densities to form general dislocation evolution equations applicable over a range of length scales. Based on basic principles in dislocation mechanics, [Bammann \(2001\)](#) and [Beaudoin and Acharya \(2001\)](#) developed an evolution equation for the SSD density that incorporates explicitly the effect of GND density, such that

$$\dot{\rho}_S = \left( k_0 \rho_G + \frac{k_1}{b} \sqrt{\rho_S} - k_2 \rho_S \right) \dot{\gamma}^P, \quad (7)$$

where  $k_0$  is a material parameter. The first term in Eq. (7) is due to entanglement of glide GNDs with the other forest dislocations identified by lattice incompatibility. The second and third terms follow exactly the development of [Kocks \(1966, 1976\)](#), [Estrin and Mecking \(1984\)](#), and [Kubin and Estrin \(1990\)](#). The generation terms dominate the evolution of dislocation density at the low dislocation density levels typical of annealed crystals at low strains. The recovery term becomes proportionally larger as the dislocation density statistically accumulates, and it controls the saturation level of the dislocation density ([Arsenlis et al., 2004](#)).

If  $L$  is the average distance traveled by a newly generated dislocation in an increment of time  $dt$ , then the rate of accumulation of plastic shear strain due to mobile dislocation density,  $\rho_m$ , scales with the Orowan relation,  $\dot{\gamma}^P dt \propto b \rho_m L$ . Assuming that the dislocation velocity between obstacles is so high that it can be neglected, the average velocity of a mobile dislocation,  $v$ , is proportional to  $L/t_w$ , where  $t_w$  is the waiting time spent at the obstacle. Then one can express  $\dot{\gamma}^P$  as

$$\dot{\gamma}^P = b \rho_m v. \quad (8)$$

Furthermore, [Bammann and Aifantis \(1982\)](#) generalized the increment in the plastic strain tensor in the macroscopic plasticity theory,  $\dot{\epsilon}_{ij}^P$ , in terms of the effective plastic shear strain increment,  $\dot{\gamma}^P$ , and the symmetric Schmidt's orientation second-order tensor,  $m_{ij}$ , as follows:

$$\dot{\epsilon}_{ij}^P = \dot{\gamma}^P m_{ij}. \quad (9)$$

In expressing the plastic strain tensor at the macro level to the plastic shear strain at the micro level, an average form of the Schmidt's tensor is assumed since plasticity at the macroscale incorporates a number of differently oriented grains into each continuum point.

The flow stress  $\sigma$  in Eq. (3) is the conjugate of the effective plastic strain variable  $\dot{\epsilon}^p = \sqrt{\frac{2}{3} \dot{\epsilon}_{ij}^p \dot{\epsilon}_{ij}^p}$  in macro-plasticity. Hence, by using Eq. (9) one can write  $\dot{\epsilon}^p$  as follows:

$$\dot{\epsilon}^p = \frac{1}{m} b \rho_m v, \tag{10}$$

where  $m = 1/\sqrt{\frac{2}{3} m_{ij} m_{ij}}$  is the Schmidt’s orientation factor or the average Taylor factor. Equivalently, one can write the relationship  $\dot{\gamma}^p = m \dot{\epsilon}^p$  that relates the effective plastic shear strain increment to the corresponding normal effective plastic strain.

It is clear from Eq. (10) that the Burgers vector and the dislocation spacing are two physical length measures which control plastic deformation.

### 3. Theory formulation

#### 3.1. Size-dependent plasticity

In this section, a nonlocal constitutive relation is developed based on the dislocation based principals outlined in the previous section. Eq. (7) is the key idea of this paper. By taking into consideration the dislocation processes of generation, motion, immobilization, recovery, and annihilation in which the GNDs contribute to the storage of SSDs, one is able to bridge the gap between continuum plasticity and dislocation-based crystal plasticity. The following guiding principles in the present gradient constitutive framework are used: (a) the flow stress obeys the Taylor hardening relation of Eq. (3); (b) the evolutions of GND and SSD densities are calculated using Eqs. (5) and (7), respectively.

Differentiating the flow stress in Eq. (3) with respect to time, one obtains

$$\dot{\sigma} = \frac{\partial \sigma}{\partial \rho_S} \dot{\rho}_S + \frac{\partial \sigma}{\partial \rho_G} \dot{\rho}_G = \frac{\partial \sigma}{\partial \rho_i} (\dot{\rho}_S + \dot{\rho}_G), \tag{11}$$

where  $\dot{\rho}_i = \dot{\rho}_S + \dot{\rho}_G$ . Substitution of the evolution equations for  $\dot{\rho}_S$  and  $\dot{\rho}_G$  from Eqs. (7) and (5), respectively, along with the relationship  $\dot{\gamma}^p = m \dot{\epsilon}^p$  yields

$$\dot{\sigma} = \frac{m \alpha G b}{2 \sqrt{\rho_i}} \left[ \left( \frac{k_0 m \bar{r}}{b} \frac{\partial \dot{\epsilon}^p}{\partial x} + \frac{k_1}{b} \sqrt{\rho_S} - k_2 \rho_S \right) m \dot{\epsilon}^p + \frac{m \bar{r}}{b} \frac{\partial \dot{\epsilon}^p}{\partial x} \right]. \tag{12}$$

Let  $\sigma_S$  be the flow stress without gradients such that one can write Eq. (3) as follows:

$$\sigma_S = \sigma_0 + m \alpha G b \sqrt{\rho_S}. \tag{13}$$

Using Eqs. (3) and (13), one can write useful equations for  $\rho_i$  and  $\rho_S$ , respectively, as follows:

$$\rho_i = \left( \frac{\sigma - \sigma_0}{m \alpha G b} \right)^2, \quad \rho_S = \left( \frac{\sigma_S - \sigma_0}{m \alpha G b} \right)^2. \tag{14}$$

Substituting the above relations into Eq. (12) yields

$$\dot{\sigma} = \frac{m^3 \alpha^2 G^2 b \bar{r}}{2(\sigma - \sigma_0)} \left( m k_0 \frac{\partial \dot{\epsilon}^p}{\partial x} \dot{\epsilon}^p + \frac{\partial \dot{\epsilon}^p}{\partial x} \right) + \left( \frac{\sigma_S - \sigma_0}{\sigma - \sigma_0} \right) \left( \frac{m^2 \alpha G k_1}{2} - \frac{k_2 m}{2} (\sigma_S - \sigma_0) \right) \dot{\epsilon}^p. \tag{15}$$

With the absence of strain gradients,  $\dot{\sigma}$  converges to  $\dot{\sigma}_s$  such that Eq. (15) reduces to

$$\dot{\sigma}_s = \frac{1}{2} [m^2 \alpha G k_1 - k_2 m (\sigma_s - \sigma_0)] \dot{\varepsilon}^p. \tag{16}$$

In order to determine the coefficients  $k_1$  and  $k_2$  that appear in the above differential equations, Eqs. (15) and (16), the strain rate hardening concept in the absence of strain gradients is used here,  $h = d\sigma_s/d\varepsilon^p$ . Thus, one can define the  $h$ – $\sigma_s$  curve using Eq. (16) as follows:

$$h = \frac{m^2 \alpha G k_1 - k_2 m (\sigma_s - \sigma_0)}{2(1 + \frac{1}{2} k_2 m \dot{\varepsilon}^p t_w)}. \tag{17}$$

Defining  $h_0$  as the strain hardening rate that prevails at initial yield ( $\varepsilon^p = 0$ ) or onset of plastic flow and the saturation stress ( $h(\sigma_s = \sigma_{sat}) = 0$ ) in the absence of gradients effects, one can express  $k_1$  and  $k_2$  with the aid of Eq. (10) as follows:

$$k_1 = \frac{2h_0}{m^2 \alpha G \Omega}, \quad k_2 = \frac{2h_0}{m(\sigma_{sat} - \sigma_0)}, \tag{18}$$

where  $\Omega = 1 - (h_0 b \rho_{m0} L)/m(\sigma_{sat} - \sigma_0)$  with  $\rho_{m0}$  is the initial mobile dislocation density. However, the work by Kubin and Estrin (1990) suggests that this value is very small (on the order of  $10^5 \text{ mm}^{-2}$  for annealed materials) and can be neglected in this work such that  $\Omega \approx 1$ . The subscript sat in Eq. (18) denotes the state at which the stress saturates, as estimated from an extrapolation of the  $h$ – $\sigma_s$  curve. The initial hardening modulus  $h_0$  and the saturated stress  $\sigma_{sat}$  are dependent on the strain rate and temperature and can be determined through routine uniaxial test data such that the effects of length scale are not significant (e.g., using the stress–strain diagrams of a course grain material).

Substituting  $k_1$  and  $k_2$  from Eq. (18) into Eq. (16) yields the flow stress relation without the presence of strain gradients as follows:

$$\dot{\sigma}_s = h_0 \left( \frac{\sigma_{sat} - \sigma_s}{\sigma_{sat} - \sigma_0} \right) \dot{\varepsilon}^p. \tag{19}$$

For uniaxial proportional loading the above equation can be integrated analytically to yield the Voce stress–strain equation

$$\sigma_s = \sigma_{sat} + (\sigma_0 - \sigma_{sat}) \exp \left( - \frac{h_0}{\sigma_{sat} - \sigma_0} \varepsilon^p \right). \tag{20}$$

Substituting  $k_1$  and  $k_2$  from Eq. (18) into Eq. (15) yields the flow stress relation with the presence of strain gradients as follows:

$$\dot{\sigma} = h_0 \left( \frac{\sigma_s - \sigma_0}{\sigma - \sigma_0} \right) \left( \frac{\sigma_{sat} - \sigma_s}{\sigma_{sat} - \sigma_0} \right) \dot{\varepsilon}^p + \frac{m^3 \alpha^2 G^2 b \bar{r}}{2(\sigma - \sigma_0)} \left( m k_0 \frac{\partial \varepsilon^p}{\partial x} \dot{\varepsilon}^p + \frac{\partial \dot{\varepsilon}^p}{\partial x} \right). \tag{21}$$

It is obvious that the above equation degenerates to Eq. (19) in the absence of gradient effects. After substituting Eq. (20), the above equation can be integrated analytically for uniaxial and proportional loading and leads to a gradient plasticity model in the form

$$\sigma = \sigma_0 + \sigma_{\text{ref}} \sqrt{f_p^2(\varepsilon^p) + \ell(\varepsilon^p)\eta^p}, \tag{22}$$

where  $\eta^p = \sqrt{\nabla_k \varepsilon^p \nabla_k \varepsilon^p}$  is the effective strain gradient and  $\sigma_{\text{ref}} = \sigma_{\text{sat}} - \sigma_0$  can be defined as the saturation value of the isotropic hardening function  $\sigma - \sigma_0$ . The nondimensional function  $f_p(\varepsilon^p)$  is obtained as a function of  $\varepsilon^p$  as

$$f_p(\varepsilon^p) = 1 - \exp\left(-\frac{h_0}{\sigma_{\text{ref}}} \varepsilon^p\right) \tag{23}$$

and

$$\ell(\varepsilon^p) = m^3 \alpha^2 b \bar{r} \left(\frac{G}{\sigma_{\text{ref}}}\right)^2 (1 + mk_0 \varepsilon^p) \tag{24}$$

is identified as the intrinsic material length scale. Beaudoin and Acharya (2001) showed that the parameter  $k_0$  accounts for the grain size dependency.

The expression for the flow stress in Eq. (22) is similar to that of the MSG and TNT plasticity theories (e.g., Nix and Gao, 1998; Gao et al., 1999a,b; Huang et al., 2000a; Gao and Huang, 2001). However, a different expression for  $\ell$  is obtained in formulating the MSG and TNT theories,  $\ell = 18\alpha^2(G/\sigma_{\text{ref}})^2 b$ , which indicates that the length scale parameter is fixed and does not change with the course of plastic deformation as suggested by Eq. (24). Voyiadjis and Abu Al-Rub (2005) show that the current gradient plasticity theories do not give sound interpretations of the size effects in micro-bending and micro-torsion tests if a definite and fixed length scale parameter is used. They showed that  $\ell$  is in the order of the average distance between dislocations (i.e., that  $\ell \propto L$ ) which depends on the grain size,  $d$ , and the effective plastic strain,  $\varepsilon^p$ . This result has been confirmed by the micro-indentation comparisons of Begley and Hutchinson (1998) and Abu Al-Rub and Voyiadjis (2004a) and by the micro-bending tests of Haque and Saif (2003). Moreover, Nix and Gao (1998) pointed out that  $\ell$  scales with  $\ell \sim L^2/b$ . However, Gracio (1994) approximated the evolution of mean dislocation spacing  $L$  as a function of the grain size,  $d$ , the effective plastic strain,  $\varepsilon^p$ , the hardening exponent,  $n$ , and the characteristic dimension of the specimen,  $D$  (usually taken as the smallest dimension, e.g., the thickness for micro-bending specimens and the diameter for micro-torsion specimens),  $L = Dd/[D + d(\varepsilon^p)^{1/n}]$ . Therefore, the material length scale in metals can be considered by itself as an internal variable representing the dislocation cell structure and grain size.

Therefore, the proposed unified expression of the flow stress in Eqs. (21)–(24) is physically sound with strong dislocation mechanics-based interpretations. Moreover, the phenomenological measure of the yield stress in uniaxial tension,  $\sigma_{\text{ref}}$ , and the microstructure length scale parameter,  $\ell$ , are now related to measurable physical parameters. Moreover, one can note that Eq. (24) implies that  $\ell$  may vary with the strain rate and temperature for a given material for the case  $\sigma_{\text{ref}}$ ,  $\sigma_0$ ,  $\sigma_{\text{sat}}$ , and  $h_0$  being dependent on strain rate and temperature. However, for most metals, the yield stress increases with the strain rate and decreases with temperature increase. This causes  $\ell$  to decrease with increasing strain rates, but to

increase with temperature decrease (Abu Al-Rub and Voyiadjis, 2004b). This is not the subject of this paper but more work needs to be done in this direction.

It is imperative to mention that, generally, there exist two frameworks of gradient plasticity theories to model size effects at the micron and sub-micron scales. The first framework involves higher-order stresses and higher-order (or additional) governing equations and therefore requires extra boundary conditions, such as the couple stress theory (e.g., Fleck and Hutchinson, 1993, 1997, 2001; Gurtin, 2002, 2003), and MSG theory. The second framework does not involve the higher-order stresses and the equilibrium equation remains the same as those of classical theory (e.g., Acharya and Bassani, 2000; Bassani, 2001; Chen and Wang, 2002; Gao and Huang, 2001; Abu Al-Rub and Voyiadjis, 2004a). Huang et al. (2000a) showed that the higher-order stresses have a little or essentially no effect on the predictions of size effects in micro-bending, micro-torsion, micro-indentation, crack-tip, void growth, etc. In fact, MSG theory was recently modified by Huang et al. (2004) such that it does not involve the higher-order stresses and therefore falls into the second category of the strain gradient plasticity that preserves the structure of conventional plasticity theories. Furthermore, Bazant and Guo (2002) argue that the asymptotic behavior at small sizes is unreasonably strong in the first category of strain gradient plasticity theories because of the presence of third-order stresses in these models. The theory presented in this paper falls in the second category, where no higher-order stresses are involved. This feature would make the strain gradient plasticity theories very attractive in applications, since higher-order boundary conditions may not be uniquely defined and/or can be difficult to satisfy if one uses the first category of strain gradient plasticity theories. Moreover, we introduce here higher-order gradients of the plasticity hardening state variable, which is the effective plastic strain,  $e^p$ , into the constitutive equation for the flow stress, while leaving all other features of classical plasticity unaltered. This is different than the MSG theory, which introduces higher-order gradients of the plastic strain tensor  $e_{ij}^p$ . Therefore, the two theories are different.

### 3.2. Deformation theory of gradient plasticity

The deformation theory of the proposed size-dependent plasticity assumes the same structure as the classical plasticity theory (Hill, 1950). The strain tensor,  $\varepsilon_{ij}$ , is decomposed into a deviatoric part,  $e'_{ij}$ , and a volumetric part,  $\varepsilon_{kk}$ , as

$$\varepsilon_{ij} = e'_{ij} + \frac{1}{3} \varepsilon_{kk} \delta_{ij}, \quad (25)$$

where  $\delta_{ij}$  is the Kronecker delta. The volumetric strain  $\varepsilon_{kk}$  is related to the hydrostatic stress  $\sigma_{kk}$  through the elastic bulk modulus  $K = E/3(1 - 2\nu)$ , where  $E$  is the Young's modulus and  $\nu$  is the Poisson's ratio, such that

$$\varepsilon_{kk} = \frac{\sigma_{kk}}{3K}. \quad (26)$$

The deviatoric strain tensor  $e'_{ij}$  is proportional to the deviatoric stress tensor  $\sigma'_{ij} = \sigma_{ij} - \frac{1}{3} \sigma_{kk} \delta_{ij}$  through the von-Mises conventional plasticity, such that

$$\dot{\epsilon}'_{ij} = \frac{3\epsilon_e}{2\sigma_e} \dot{\sigma}'_{ij}, \tag{27}$$

where  $\epsilon_e = \sqrt{\frac{2}{3}\dot{\epsilon}'_{ij}\dot{\epsilon}'_{ij}}$  is the effective strain and  $\sigma_e = \sqrt{\frac{3}{2}\dot{\sigma}'_{ij}\dot{\sigma}'_{ij}}$  is the effective stress.

The yield criterion is the same as given in Eq. (22), but the flow stress is set equal to the effective stress, i.e.,  $\sigma = \sigma_e$ , and re-written in terms of the effective strain  $\epsilon_e$  and the effective strain gradient  $\eta = \sqrt{\nabla_k \epsilon_e \nabla_k \epsilon_e}$  such that

$$\sigma_e = \sigma_0 + \sigma_{ref} \sqrt{f^2(\epsilon_e) + \ell(\epsilon_e)\eta}. \tag{28}$$

Combining the above relations leads to the following constitutive equations for the deformation theory of the current gradient plasticity:

$$\sigma_{kk} = 3K\epsilon_{kk}, \quad \dot{\sigma}'_{ij} = \frac{2(\sigma_0 + \sigma_{ref} \sqrt{f^2(\epsilon_e) + \ell(\epsilon_e)\eta})}{3\epsilon_e} \dot{\epsilon}'_{ij}, \tag{29}$$

where  $\ell(\epsilon_e) = m^3 \alpha^2 b \bar{r} (G/\sigma_{ref})^2 (1 + mk_0 \epsilon_e)$  is given in Eq. (24) and  $f(\epsilon_e)$  could be taken as a power law  $f(\epsilon_e) = \epsilon_e^{1/n}$ , where  $n \geq 1$  is the work hardening exponent.

### 3.3. $J_2$ flow theory of gradient plasticity

In the flow theory of the present gradient plasticity, the constitutive equations are expressed in rate form. The strain rates can be decomposed into a deviatoric part and a volumetric part as follows:

$$\dot{\epsilon}_{ij} = \dot{\epsilon}'_{ij} + \frac{1}{3} \dot{\epsilon}_{kk} \delta_{ij}, \tag{30}$$

where the volumetric strain rate is purely elastic and is related to the hydrostatic stress rate  $\dot{\sigma}_{kk}$  as

$$\dot{\epsilon}_{kk} = \frac{\dot{\sigma}_{kk}}{3K}. \tag{31}$$

The deviatoric strain rate,  $\dot{\epsilon}'_{ij}$ , consists of an elastic part,  $\dot{\epsilon}'_{ij}{}^e$ , and a plastic part,  $\dot{\epsilon}'_{ij}{}^p$ , such that

$$\dot{\epsilon}'_{ij} = \dot{\epsilon}'_{ij}{}^e + \dot{\epsilon}'_{ij}{}^p, \tag{32}$$

where  $\dot{\epsilon}'_{kk}{}^p = 0$  and the elastic strain rate  $\dot{\epsilon}'_{ij}{}^e$  is proportional to the deviatoric stress rate  $\dot{\sigma}'_{ij} = \dot{\sigma}_{ij} - \frac{1}{3} \dot{\sigma}_{kk} \delta_{ij}$  through the shear modulus  $G = E/2(1 + \nu)$ ,

$$\dot{\epsilon}'_{ij}{}^e = \frac{\dot{\sigma}'_{ij}}{2G}. \tag{33}$$

The yield criterion is the same as that given in Eq. (22) such that

$$f = \sigma_e - \sigma_0 - \sigma_{ref} \sqrt{f_p^2(\epsilon^p) + \ell(\epsilon^p)\eta^p} \equiv 0, \tag{34}$$

where  $\sigma_e = \sqrt{\frac{3}{2}\dot{\sigma}'_{ij}\dot{\sigma}'_{ij}}$  is the effective stress and  $f_p(\epsilon^p)$  and  $\ell(\epsilon^p)$  are given by Eqs. (23) and (24), respectively.

The plastic strain rate  $\dot{\epsilon}'_{ij}{}^p$  is proportional to the deviatoric stress  $\sigma'_{ij}$  by the normality flow rule

$$\dot{\epsilon}_{ij}^p = \dot{\epsilon}^p \frac{\partial f}{\partial \sigma_{ij}} = \frac{3\dot{\epsilon}^p}{2\sigma_e} \sigma'_{ij}, \tag{35}$$

where  $\dot{\epsilon}^p = \sqrt{\frac{2}{3} \dot{\epsilon}_{ij}^p \dot{\epsilon}_{ij}^p}$  is the effective plastic strain rate. Combining Eqs. (32)–(35) yields

$$\dot{\sigma}'_{ij} = 2G \left( \dot{\epsilon}'_{ij} - \frac{3\dot{\epsilon}^p}{2\sigma_e} \sigma'_{ij} \right). \tag{36}$$

For the classical plasticity (i.e., plasticity with the absence of strain gradients), one can re-write the Voce stress–strain relation that appears in Eq. (20) as follows:

$$\sigma_s = \sigma_0 + \sigma_{ref} f_p(\epsilon^p), \tag{37}$$

where  $f_p(\epsilon^p)$  is given by Eq. (23). Moreover, by combining Eqs. (21), (24) and (37), one can re-write the rate of the flow stress as

$$\dot{\sigma}_e = \frac{\sigma_{ref}}{2(\sigma_e - \sigma_0)} \left[ (2f_p f'_p + \ell' \eta^p) \dot{\epsilon}^p + \ell \left( \frac{\dot{\eta}^p}{1 + mk_0 \epsilon^p} \right) \right], \tag{38}$$

where the gradient variable  $\dot{\eta}^p$  is given by

$$\dot{\eta}^p = \frac{\nabla_k \epsilon^p \nabla_k \dot{\epsilon}^p}{\eta^p} \tag{39}$$

and  $f'_p = \partial f_p / \partial \epsilon^p$  and  $\ell' = \partial \ell / \partial \epsilon^p$  are obtained from Eqs. (23) and (24), respectively, as

$$f'_p = \frac{h_0}{\sigma_{ref}} (1 - f_p), \quad \ell' = m^4 \alpha^2 b \bar{r} \left( \frac{G}{\sigma_{ref}} \right)^2 k_0. \tag{40}$$

Differentiating the square of  $\sigma_e = \sqrt{\frac{3}{2} \sigma'_{ij} \sigma'_{ij}}$  with respect to time gives the consistency condition

$$2\sigma_e \dot{\sigma}_e = 3\sigma'_{ij} \dot{\sigma}'_{ij} \tag{41}$$

Inserting Eqs. (36) and (38) into the above equation leads to

$$\dot{\epsilon}^p = \frac{6G \left( \frac{\sigma_e - \sigma_0}{\sigma_e} \right) \sigma'_{ij} \dot{\epsilon}'_{ij} - \sigma_{ref}^2 \ell \left( \frac{\dot{\eta}^p}{1 + mk_0 \epsilon^p} \right)}{6G(\sigma_e - \sigma_0) + \sigma_{ref}^2 (2f_p f'_p + \ell' \eta^p)}. \tag{42}$$

Finally, the constitutive equations for the flow theory of the present gradient plasticity are assembled as follows

$$\dot{\sigma}_{kk} = 3K \dot{\epsilon}_{kk} \tag{43}$$

$$\dot{\sigma}'_{ij} = \begin{cases} 2G \left[ \dot{\epsilon}'_{ij} - \frac{3}{2} \frac{\sigma'_{ij}}{\sigma_e} \frac{6G \left( \frac{\sigma_e - \sigma_0}{\sigma_e} \right) \sigma'_{mn} \dot{\epsilon}'_{mn} - \sigma_{ref}^2 \ell \left( \frac{\dot{\eta}^p}{1 + mk_0 \epsilon^p} \right)}{6G(\sigma_e - \sigma_0) + \sigma_{ref}^2 (2f_p f'_p + \ell' \eta^p)} \right] & \text{if } f = 0 \quad \text{and} \quad \dot{\sigma}_e \geq 0, \\ 2G \dot{\epsilon}'_{ij} & \text{if } f < 0 \quad \text{and} \quad \dot{\sigma}_e < 0. \end{cases} \tag{44}$$

It is emphasized that under proportional deformation, it can be shown that the deformation theory presented in Section 3.2 coincides with the flow theory. Moreover, the consistency condition in the classical flow theory is used to derive a point-wise relation between stress rate and strain rate, whereas the current gradient theory has a nonlocal relation between the stress rates and strain rates.

#### 4. Applications

This section presents some recent applications of gradient plasticity to handle size effects observed in metals. We will use the proposed gradient plasticity theory presented in Section 3 to investigate the size-dependent behavior in micro-bending of thin films, micro-torsion of thin wires, and micro-indentation.

##### 4.1. Micro-bending of thin films

Stolken and Evans (1998), Shrotriya et al. (2003), and Haque and Saif (2003) performed bending tests of thin films with different thicknesses and observed that the bending strength of beams significantly decreased with the beam thickness increase. This size effect cannot be explained using the classical plasticity theory which does not possess an intrinsic material length scale. In this section, due to the postulated proportional loading in the bending problem, we will use the deformation theory of gradient plasticity presented in Section 3.2 to investigate the strength of thin beams in pure bending. For simplicity, we assume that the beam is under plane-strain deformation and we neglect the elastic deformation such that the material is incompressible. Accordingly, no distinction is made between  $\varepsilon_{ij}$  and  $\varepsilon'_{ij}$ .

Let  $x_1$  be the neutral axis of the beam and the bending occurs in the  $x_1$ – $x_2$  plane. The curvature of the beam is designated as  $\kappa$ , the thickness is  $h$ , and the width in the out-of-plane ( $x_3$ ) direction is  $b$ . From classical strength of materials, the displacement field of the beam under plane-strain bending (the out-of-plane width in the  $x_3$  direction is much larger than the thickness in the  $x_2$  direction) can be defined as follows:

$$u_1 = -\kappa x_1 x_2, \quad u_2 = -\kappa(x_1^2 + x_2^2)/2, \quad u_3 = 0. \tag{45}$$

The associated nonvanishing strain components are given by:

$$\varepsilon_{11} = -\varepsilon_{22} = \kappa x_2, \quad \varepsilon_{12} = 0. \tag{46}$$

In the deformation theory of plasticity there is no formal distinction between elastic and plastic components of strain and the change in the plastic strain can be formally integrated. We can then express the effective strain,  $\varepsilon_e = \sqrt{\frac{2}{3} \varepsilon_{ij} \varepsilon_{ij}}$ , and the effective strain gradients,  $\eta = \sqrt{\nabla_k \varepsilon_e \nabla_k \varepsilon_e}$ , using Eq. (46) as follows:

$$\varepsilon_e = \frac{2}{\sqrt{3}} \kappa |x_2|, \quad \eta = \frac{2}{\sqrt{3}} \kappa. \tag{47}$$

The nonvanishing deviatoric stresses can be obtained from Eq. (29)<sub>2</sub> as

$$\sigma'_{11} = -\sigma'_{22} = \frac{\sigma_e}{\sqrt{3}} \frac{x_2}{|x_2|}. \tag{48}$$

The nonvanishing stresses,  $\sigma_{ij} = \sigma'_{ij} + \frac{1}{3}\sigma_{kk}\delta_{ij}$  with  $\sigma_{kk} = 3\sigma'_{11}$ , can be expressed as:

$$\sigma_{11} = \frac{2\sigma_e}{\sqrt{3}} \frac{x_2}{|x_2|}, \quad \sigma_{33} = \frac{\sigma_e}{\sqrt{3}} \frac{x_2}{|x_2|}, \tag{49}$$

where the flow stress in a power-law hardening material, can be expressed by substituting Eqs. (47) into Eq. (28), as follows:

$$\sigma_e = \sigma_0 + \sigma_{\text{ref}} \sqrt{\left(\frac{2}{\sqrt{3}}\kappa|x_2|\right)^{2/n} + \frac{2\ell_0}{\sqrt{3}}\left(1 + \frac{2mk_0}{\sqrt{3}}\kappa|x_2|\right)\kappa}, \tag{50}$$

where  $\ell_0 = m^3\alpha^2 b\bar{r}(G/\sigma_{\text{ref}})^2$  is the initial value of the material length scale (i.e., when  $\varepsilon_e = 0$ ). The pure bending moment  $M$  can be determined from the integration of the normal stress  $\sigma_{11}$  in Eq. (49)<sub>1</sub> over the cross-section of the beam as:

$$M = \frac{2b}{\sqrt{3}} \int_{-h/2}^{h/2} \sigma_e|x_2| dx_2. \tag{51}$$

Substituting Eq. (50) into the above equation with the aid of variable substitution (i.e.,  $y = x_2/h$ ), it follows:

$$\frac{M}{bh^2} = \frac{\sigma_0}{2\sqrt{3}} + \frac{4\sigma_{\text{ref}}}{\sqrt{3}} \int_0^{0.5} \left[ \left(\frac{4}{\sqrt{3}}\varepsilon_s y\right)^{2/n} + \frac{4\beta\varepsilon_s}{\sqrt{3}} \left(1 + \frac{4mk_0}{\sqrt{3}}\varepsilon_s y\right) \right]^{1/2} y dy, \tag{52}$$

where  $\varepsilon_s = \kappa h/2$  is the surface curvature and  $\beta = \ell_0/h$ . In the limit of  $h \gg \ell_0$ ,  $M$  degenerates to that for classical plasticity, such that:

$$\frac{M_0}{bh^2} = \frac{M_0}{bh^2} (\ell_0 \rightarrow 0 \text{ and } k_0 \rightarrow 0) = \frac{\sigma_0}{2\sqrt{3}} + c(\varepsilon_s)^{1/n} \quad \text{with } c = \frac{2^{1/n}n\sigma_{\text{ref}}}{3^{(n+1)/2n}(2n+1)}. \tag{53}$$

Note that the moment–curvature relation in Eq. (52) differs from the corresponding result for MSG plasticity derived by Huang et al. (2000a). This difference stems out from the presence of higher-order stresses in the MSG plasticity which is already proved by Huang et al. (2004) that the moment–curvature relation is insensitive to the presence of these higher-order stresses. Moreover, this moment–curvature relation differs from the corresponding result of TNT plasticity derived by Gao and Huang (2001) due to the dependence of the length scale in the present gradient plasticity on the strain accumulation and on the grain size, Eq. (24).

In order to check the predictions of the present gradient plasticity with experimental results at the micron scale, use is made of three sets of micro-bending tests reported by Stolken and Evans (1998) for bending of thin 99.994% pure Annealed Nickel films, Shrotriya et al. (2003) for bending of thin LIGA Nickel films, and Haque and Saif (2003) for bending of nano 99.999% pure Aluminum films. Note that it

was reported in these tests that no damage occurred in the material such that the measured strength data provides a true measure of the plastic properties of the specimen. Micro-bending thus provide a convenient tool for the identification of the plasticity intrinsic material length scale, when damage is avoided.

Fig. 1 compares the predictions from the present gradient plasticity with the micro-bending test of thin Ni films by Stolken and Evans (1998), with foil width  $b = 2.5$  mm, length  $L = 6$  mm, and thicknesses  $h = 12.5, 25,$  and  $50 \mu\text{m}$ . The experimental results are fitted with  $\sigma_{\text{ref}} = 1167$  MPa,  $G = 84$  GPa,  $n = 1$ , and  $\sigma_0 = 103, 75, 56$  MPa for  $h = 12.5, 25,$  and  $50 \mu\text{m}$ , respectively. The microstructural parameters associated with the evolution of the length scale in Eq. (24) are  $m = 3.08, \bar{r} = 1.85, b = 0.25$  nm,  $k_0 = 2.5$ , and  $\alpha = 0.3$  which produces an expression for the length scale  $\ell = 6.3(1 + 7.7\epsilon_e) \mu\text{m}$  with an initial value of  $\ell_0 = 6.3 \mu\text{m}$ . The parameter  $\alpha$  estimated from the experimental data has the correct order of magnitude. Stolken and Evans (1998) used an average value of the material length scale of  $\ell = 5.2 \mu\text{m}$  to fit these results; however, their fit is not as good as shown in Fig. 1.

Fig. 2 compares the predictions from the present gradient plasticity with the micro-bending test of thin LIGA Ni foils by Shrotriya et al. (2003), with foil width  $b = 0.2$  mm, length  $L = 1.50$  mm, and thickness  $h = 25, 50, 100,$  and  $200 \mu\text{m}$ . The experimental results are fitted with  $\sigma_{\text{ref}} = 1030$  MPa,  $G = 63.5$  GPa,  $n = 1$ , and  $\sigma_0 = 400, 305, 218, 191$  MPa for  $h = 25, 50, 100,$  and  $200 \mu\text{m}$ , respectively. Different values for  $\sigma_0$  are used for different sizes in order to include the so-called Hall-Petch behavior. The microstructural parameters associated with the evolution of the length scale in Eq. (24) are  $m = 3.08, \bar{r} = 1.85, b = 0.25$  nm,  $k_0 = 3.0$ , and  $\alpha = 0.5$  which produces an expression for the length scale  $\ell = 12.84(1 + 9.24\epsilon_e) \mu\text{m}$  with an initial value  $\ell_0 = 12.84 \mu\text{m}$ . Again the parameter  $\alpha$  estimated from the experimental data

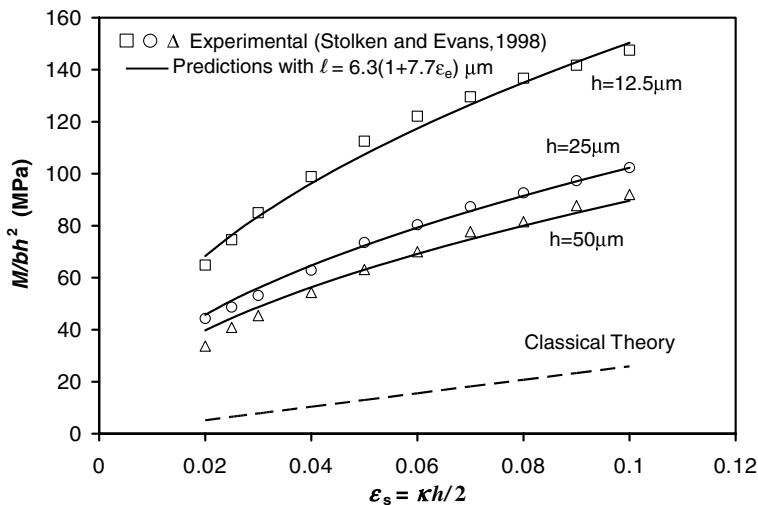


Fig. 1. Comparison of the present gradient theory with the micro-bending experiment of annealed nickel thin beams by Stolken and Evans (1998). The dashed line is the predictions if the strain gradient effects are neglected.

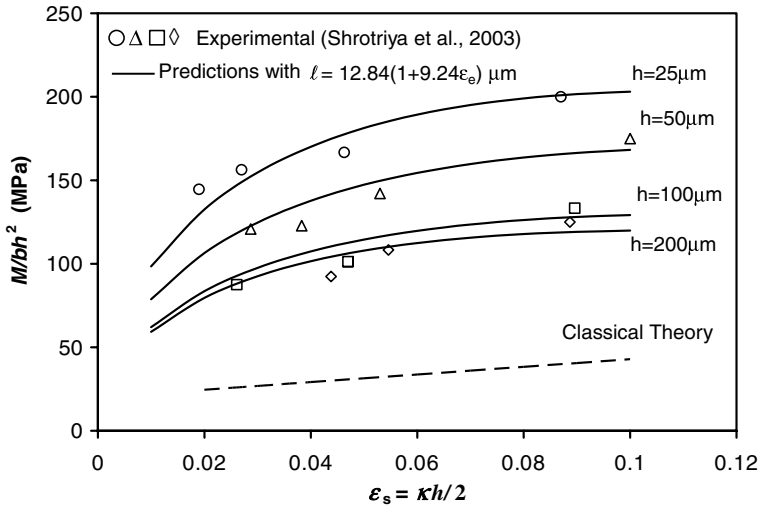


Fig. 2. Comparison of the present gradient theory with the micro-bending experiment of LIGA nickel thin films by Shrotriya et al. (2003). The dashed line is the predictions if the strain gradient effects are neglected.

has the correct order of magnitude. Shrotriya et al. (2003) used an average value of the material length scale of  $\ell = 5.6 \mu\text{m}$  to fit these results; however, their fit is very poor compared to the one that is shown in Fig. 2.

Fig. 3 compares the predictions from the present gradient plasticity with the micro-bending test of thin 99.99% pure aluminum films by Haque and Saif (2003), with film width  $b = 10 \mu\text{m}$ , length  $L = 275 \mu\text{m}$ , and thicknesses  $h = 0.1, 0.2,$  and  $0.485 \mu\text{m}$ . The experimental results are fitted with  $\sigma_{\text{ref}} = 5717 \text{ MPa}$ ,  $G = 28.5 \text{ GPa}$ ,  $n = 2.22$ , and  $\sigma_0 = 0 \text{ MPa}$ . The microstructural parameters associated with the evolution of the length scale in Eq. (24) are  $m = 3.08$ ,  $\bar{r} = 1.85$ ,  $b = 0.286 \text{ nm}$ ,  $k_0 = 5.0$ , and  $\alpha = 1.2$  which produces an expression for the length scale  $\ell = 0.55(1 + 15.4\epsilon_e) \mu\text{m}$  with an initial value  $\ell_0 = 0.55 \mu\text{m}$ . Also, Haque and Saif (2003) used different values of  $\ell$  to fit their experimental data, which confirms our previous conclusion that  $\ell$  is not a fixed parameter but it depends on the evolution of the material microstructure.

#### 4.2. Micro-torsion of thin wires

A systematic experiment in reference to the size dependence of material behavior in micro-torsion of high-purity thin copper wires has been reported by Fleck et al. (1994) even though the experiments has never been repeated. In these experiments, it is observed that the scaled shear strength increases by a factor of 3 as the wire diameter decreases from 170 to 12  $\mu\text{m}$ . However, Fleck et al. (1994) observed that in simple tension tests the corresponding increase in work-hardening with decrease of wire size is negligible. This size effect in torsion cannot be explained by the classical continuum plasticity theory, which possesses no intrinsic material length scale.

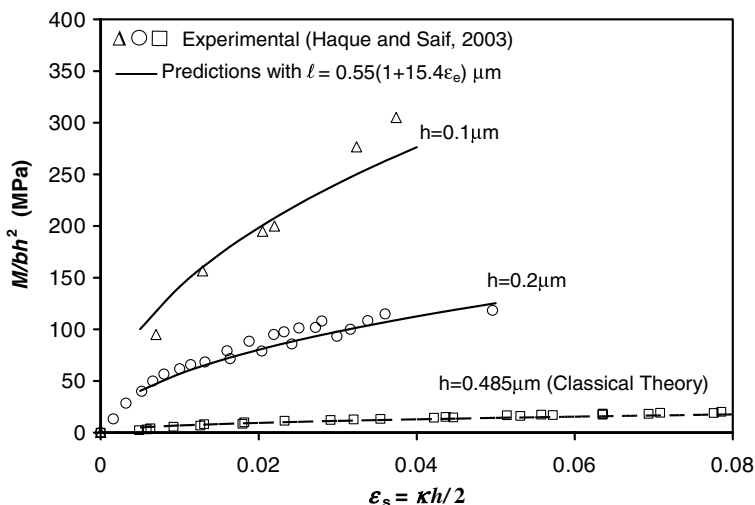


Fig. 3. Comparison of the present gradient theory with the micro-bending experiment of aluminum thin films by Haque and Saif (2003). The dashed line is the predictions if the strain gradient effects are neglected.

In this section, due to the postulated proportional loading in the torsion problem, one can use the deformation theory of the present gradient plasticity presented in Section 3.2 to investigate the strength of thin wires in torsion.

The Cartesian reference frame is set such that the  $x_1$  and  $x_2$  are in the plane of the cross-section of the wire, and the  $x_3$  axis coincides with the central axis of the wire. The twist per unit length is designated  $\kappa$  and the radius of the wire is  $a$ . The displacement field as in the classical torsion problem can be assumed as follows:

$$u_1 = -\kappa x_2 x_3, \quad u_2 = -\kappa x_1 x_3, \quad u_3 = 0. \tag{54}$$

The associated strain components are given by:

$$\epsilon_{13} = \epsilon_{31} = -\frac{1}{2}\kappa x_2, \quad \epsilon_{23} = \epsilon_{32} = \frac{1}{2}\kappa x_1, \quad \epsilon_{11} = \epsilon_{22} = \epsilon_{33} = 0, \tag{55}$$

where the strain field is obtained by adopting the assumption of incompressibility. One can express the local effective strain,  $\epsilon_e$ , and the effective strain gradient,  $\eta$ , as follows:

$$\epsilon_e = \frac{1}{\sqrt{3}}\kappa r, \quad \eta = \frac{1}{\sqrt{3}}\kappa, \tag{56}$$

where  $r = \sqrt{x_1^2 + x_2^2}$  is the radius in polar coordinates  $(r, \theta, z)$ . Eq. (29) gives the non-vanishing deviatoric stresses with  $\sigma_{kk} = 0$  as follows:

$$\sigma'_{13} = \sigma'_{31} = -\frac{\sigma_e}{\sqrt{3}}\kappa \frac{x_2}{r}, \quad \sigma'_{23} = \sigma'_{32} = \frac{\sigma_e}{\sqrt{3}}\kappa \frac{x_1}{r}, \tag{57}$$

where the flow stress in a power-law hardening material can be expressed by substituting Eq. (56) into Eq. (28) as follows:

$$\sigma_e = \sigma_0 + \sigma_{\text{ref}} \sqrt{\left(\frac{1}{\sqrt{3}} \kappa r\right)^{2/n} + \frac{\ell_0}{\sqrt{3}} \left(1 + \frac{mk_0}{\sqrt{3}} \kappa r\right) \kappa}, \tag{58}$$

where  $\ell_0 = m^3 \alpha^2 b \bar{r} (G/\sigma_{\text{ref}})^2$ . The torque can be obtained from the integration over the cross-section of the torques induced by the shear stresses  $\sigma'_{13}$  and  $\sigma'_{23}$  as

$$Q = \frac{2\pi}{\sqrt{3}} \int_0^a \sigma_e r^2 dr. \tag{59}$$

Substituting Eq. (58) into the above equation with the aid of variable substitution (i.e.,  $y = r/a$ ), it follows:

$$\frac{Q}{a^3} = \frac{2\pi}{\sqrt{3}} \left\{ \frac{\sigma_0}{3} + \sigma_{\text{ref}} \int_0^1 \left[ \left(\frac{1}{\sqrt{3}} \varepsilon_s y\right)^{2/n} + \frac{\beta \varepsilon_s}{\sqrt{3}} \left(1 + \frac{mk_0}{\sqrt{3}} \varepsilon_s y\right) \right]^{1/2} \right\} y^2 dy, \tag{60}$$

where  $\varepsilon_s = \kappa a$  is the surface angle of twist and  $\beta = \ell_0/a$ . In the limit of  $a \gg \ell_0$ ,  $Q$  degenerates to that for classical plasticity, such that

$$\frac{Q}{a^3} = \frac{Q}{a^3} (\ell_0 \rightarrow 0 \text{ and } k_0 \rightarrow 0) = \frac{2\pi\sigma_0}{3\sqrt{3}} + c(\varepsilon_s)^{1/n} \quad \text{with} \quad c = \frac{2\pi n \sigma_{\text{ref}}}{3^{(n+1)/2n} (3n+1)}. \tag{61}$$

The torque–twist relation in Eq. (60) differs from the corresponding equation for MSG plasticity derived by Huang et al. (2000a) and TNT plasticity derived by Gao and Huang (2001) for the same reasons outlined in Section 4.1.

Fig. 4 compares the predictions of the present gradient plasticity theory with the micro-torsion test of thin Copper wires by Fleck et al. (1994), with wire diameters  $2a = 12, 15, 20, 30,$  and  $170 \mu\text{m}$ . The experimental results are fitted with  $\sigma_{\text{ref}} = 226 \text{ MPa}$ ,  $G = 44 \text{ GPa}$ ,  $n = 5$ , and  $\sigma_0 = 0 \text{ MPa}$ . In these experiments, the Hall-Petch behavior of  $\sigma_0$  is not significant as reported by Fleck et al. (1994). The microstructural parameters associated with the evolution of the length scale in Eq. (24) are  $m = 3.08$ ,  $\bar{r} = 1.93$ ,  $b = 0.255 \text{ nm}$ ,  $k_0 = 3.0$ , and  $\alpha = 0.1$  which produces an expression for the length scale  $\ell = 5.45(1 + 9.24\varepsilon_e) \mu\text{m}$  with an initial value  $\ell_0 = 5.45 \mu\text{m}$ .

Fleck et al. (1994) found a range of 2.6–5.1  $\mu\text{m}$  for  $\ell$  that fitted well these experimental data and assumed that a mean value of 3.7  $\mu\text{m}$  should be satisfactory to refit these data. It is noted that better predictions were obtained by Fleck et al. (1994) model than the present model and the MSG and TNT models. This result is also obtained by Voyiadjis and Abu Al-Rub (2005) and they found that the discrepancy between the predictions from MSG plasticity and this experiment is attributed to the coupling between the local term  $f_p$  and the gradient term  $\ell \eta^p$  in Eq. (22). This coupling is assessed by the interaction between the densities of the SSDs and GNDs in the Taylor-type description of the microscopic flow stress, Eq. (3). Fleck et al. (1994) model assume a mathematical expression for this coupling in the form of a simple harmonic sum  $\sqrt{\rho_s^2 + \rho_G^2}$ , while a linear coupling in the form of  $\rho_s + \rho_G$  is assumed in formulating the present gradient plasticity and the MSG and TNT plasticity.

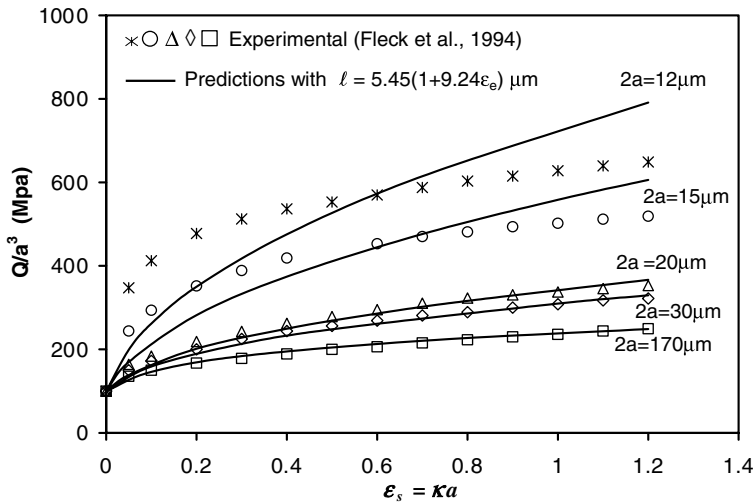


Fig. 4. Comparison of the present gradient theory with the micro-torsion experiment of copper thin wires by Fleck et al. (1994).

Moreover, since the exact form of coupling between strain hardening and strain gradient hardening is not known, Abu Al-Rub and Voyiadjis (2004a,b) and Voyiadjis and Abu Al-Rub (2005) assumed a dislocation-based coupling in the form of  $[(b^2\rho_S)^{\gamma_1} + (b^2\rho_G)^{\gamma_2}]^{1/\gamma_3}$  where  $\gamma_1$ ,  $\gamma_2$ , and  $\gamma_3$  are termed there as *interaction coefficients*. They found that setting  $\gamma_1 = \gamma_2 = \gamma_3 = 1$  gives excellent agreement between the predictions and the experiment for micro-bending and  $\gamma_1 = \gamma_2 = \gamma_3 = 2$  for micro-torsion. Therefore, the simple superposition of the density of GNDs on the density of SSDs is not well founded as also inferred by Mughrabi (2001). This subject is the focus of a current work by the authors, where the idea of the *interaction coefficients* is explored and implemented in the present framework.

#### 4.3. Micro-indentation

It is well-known by now that the hardness values from micro-indentation of metallic materials displays strong size effect. Indentation tests at scales on the order of a micron or a submicron have shown that measured hardness increases significantly with decreasing indent size (e.g., Stelmashenko et al., 1993; DeGuzman et al., 1993; Ma and Clarke, 1995; Poole et al., 1996; McElhaney et al., 1998; Lim and Chaudhri, 1999; Elmustafa and Stone, 2002; Swadener et al., 2002). Abu Al-Rub and Voyiadjis (2004a,b) presented a thorough discussion on the interpretation of the indentation size effect from conical/pyramidal (Berkovich and Vickers) and spherical indenters. In the following application, we wish to assess the predictive capability of the model presented herein to describe such a size effect.

Finite element method has been developed for the gradient plasticity theory. This method is detailed in Abu Al-Rub and Voyiadjis (2005) and Voyiadjis and Abu

Al-Rub (in press). However, in this section we use the same indentation model of Begley and Hutchinson (1998) to simulate micro-indentation experiments with the flow theory of the present gradient plasticity. Readers are referred to the above paper for details.

The material properties for cold-worked polycrystalline copper are taken from the micro-indentation experiments of McElhaney et al. (1998) by Vickers indenter:  $\sigma_{ref} = 408$  MPa,  $G = 42$  GPa,  $\nu = 0.3$ ,  $n = 3.33$ ,  $h_0 = 16$  GPa, and  $\sigma_0 = 0$  MPa. The microstructural parameters associated with the evolution of the length scale in Eq. (24) are  $m = 3.08$ ,  $\bar{r} = 2$ ,  $b = 0.255$  nm,  $k_0 = 1.5$ , and  $\alpha = 0.2$  which produces an expression for the length scale  $\ell = 6.32(1 + 4.62e^P)$   $\mu\text{m}$  with an initial value  $\ell_0 = 6.32$   $\mu\text{m}$ , which is within the findings from micro-torsion for polycrystal copper. Fig. 5 presents the micro-indentation hardness predicted by the present gradient plasticity versus the indentation depth. Fig. 5 shows that the numerically predicted hardness based on the present gradient plasticity agree remarkably well with the experimentally measured micro-indentation hardness data. The classical plasticity theory leads to a constant hardness of 0.834 GPa.

Fig. 6 compares the predictions with the micro-indentation test of Poole et al. (1996) for annealed polycrystalline copper. Here, we have taken the following material properties:  $\sigma_{ref} = 283$  MPa,  $G = 42$  GPa,  $\nu = 0.3$ ,  $n = 5$ ,  $h_0 = 11.5$  GPa, and  $\sigma_0 = 0$  MPa. The microstructural parameters associated with the evolution of the length scale in Eq. (24) are  $m = 3.08$ ,  $\bar{r} = 2$ ,  $b = 0.25$  nm,  $k_0 = 2.0$ , and  $\alpha = 0.1$  which produces an expression for the length scale  $\ell = 3.22(1 + 6.16e^P)$   $\mu\text{m}$  with an initial value  $\ell_0 = 3.22$   $\mu\text{m}$ . Excellent agreement is shown between the predictions and the experiment over a wide range of indentation depths, from 1  $\mu\text{m}$  to several micrometers. The classical plasticity theory yields a constant hardness of 0.35 GPa.

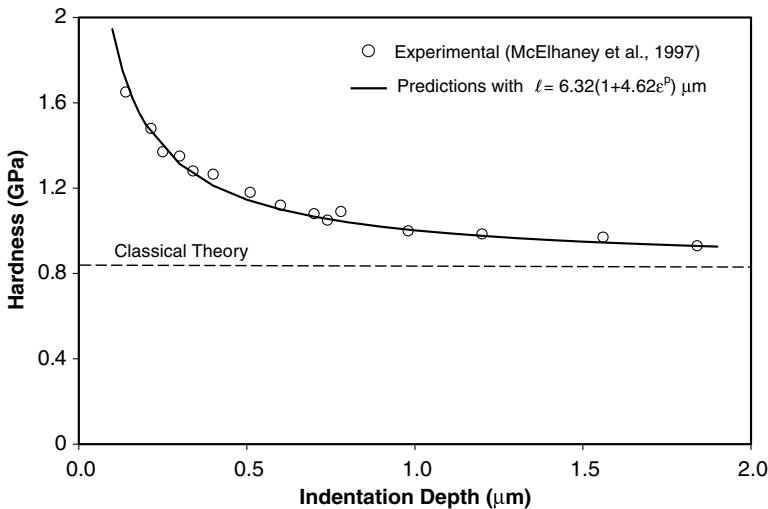


Fig. 5. Comparison of the present gradient theory with the micro-indentation experiment for cold-worked polycrystalline copper by McElhaney et al. (1998). The dashed line is the predictions if the strain gradient effects are neglected.

It can be seen from the results in Figs. 5 and 6 that as the depth of indentation  $h$  becomes much larger than  $\ell$ , the gradient effects become smaller and the corresponding hardness degenerates to the hardness in classical plasticity.

Moreover, the effect of the friction stress or the intrinsic lattice resistance,  $\sigma_0$ , on the material behavior at the microscale is explicitly considered in predicting the experimental results for nickel in Figs. 1 and 2, where different values of  $\sigma_0$  are used for different sizes. This variation in  $\sigma_0$  is attributed to the grain size effect or the so-called Hall-Petch behavior. The proposed gradient plasticity theory cannot capture size effects encountered in uniaxial tests of polycrystalline materials since the macroscopic gradients vanish and a homogeneous plastic strain field reveals and hence the constitutive gradient-dependence would have no influence. Modifications of the proposed gradient plasticity in order to include the scale-dependence of the initial yield strength  $\sigma_0$  can be achieved by incorporating the role of interfaces between grains in enhancing the yield strength of polycrystals. The current gradient plasticity theory can be enhanced by the introduction of an interfacial energy that incorporates the local plastic strain gradients at the interfaces due to dislocation pile-ups. Another way to include the size effect in  $\sigma_0$  is by using the current gradient plasticity theory in a crystal plasticity framework where the jumps in plastic strain at the interfaces of the grain boundaries are explicitly accounted for. Initial attempts in these directions have been made by Acharya and Beaudoin (2000), Qiu et al. (2001), Arsenlis et al. (2004), Evers et al. (2004), and Aifantis and Willis (2005). However, more studies are needed to explore the effect of the friction stress or the intrinsic lattice resistance on the material behavior at the microscale.

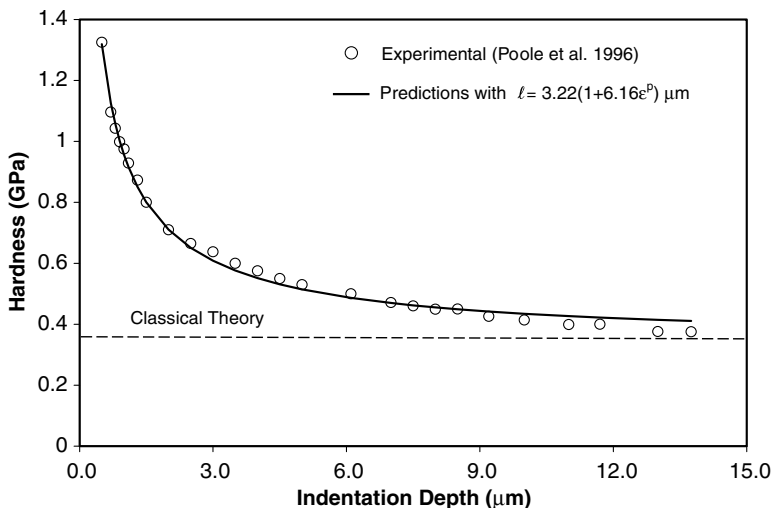


Fig. 6. Comparison of the present gradient theory with the micro-indentation experiment for annealed polycrystalline copper by Poole et al. (1996). The dashed line is the predictions if the strain gradient effects are neglected.

## 5. Conclusions

In this work a gradient plasticity theory, which bridges the gap between continuum and dislocation-based theories, is developed. This theory is based on the Taylor's dislocation hardening model that incorporates evolution equations of SSD and GND densities and assumes a simple addition of the densities from SSDs and GNDs. The key idea of this paper is the consideration of dislocation processes of generation, motion, immobilization, recovery, and annihilation in which the GNDs contribute to the storage of SSDs. These features are not considered explicitly in formulating the current macroscopic gradient plasticity theories (e.g., the works of Aifantis and co-workers, Fleck and co-workers, and Gao and co-workers). Moreover, the proposed theory falls within the essential structure of classical plasticity theories.

For proportional and monotonic loadings, the expression for the flow stress is similar to that of the MSG and TNT plasticity theories. However, a different expression for the material length scale parameter,  $\ell$ , is obtained which indicates that the length scale parameter is not fixed and changes with the course of plastic deformation and grain size. Therefore, the material length scale in metals can be considered by itself as an internal variable representing the dislocation cell structure and grain size.

The proposed model is used to investigate the micro-bending of thin beams, micro-torsion of thin wires, and indentation size effect. The proposed theory provides accurate predictions when compared to the experimental results.

The results from micro-torsion predictions indicate that, in the Taylor-type descriptions of the macroscopic flow stress, the simple superposition of the density of GNDs on the density of SSDs is not well founded. Therefore, more work is needed to investigate the proper coupling between strain hardening and strain gradient hardening. This requires elucidation from well designed experiments, physical continuum theories at the single crystal level, and dislocation mechanics.

## Acknowledgments

The authors gratefully acknowledge the financial support by the Air Force Institute of Technology, WPAFB, Ohio. The authors acknowledge the financial support under Grant No. M67854-03-M-6040 provided by the Marine Corps Systems Command, AFSS PGD, Quantico, Virginia. They thankfully acknowledge their appreciation to Howard "Skip" Bayes, Project Director.

## References

- Abu Al-Rub, R.K., Voyiadjis, G.Z., 2004a. Analytical and experimental determination of the material intrinsic length scale of strain gradient plasticity theory from micro- and nano-indentation experiments. *Int. J. Plasticity* 20, 1139–1182.

- Abu Al-Rub, R.K., Voyiadjis, G.Z., 2004b. Determination of the material intrinsic length scale of gradient plasticity theory. *Int. J. Multiscale Comput. Eng.* 2 (3), 47–70.
- Abu Al-Rub, R.K., Voyiadjis, G.Z., 2005. A direct finite element implementation of the gradient plasticity theory. *Int. J. Numer. Meth. Eng.* 63, 603–629.
- Acharya, A., Bassani, J.L., 2000. Lattice incompatibility and a gradient theory of crystal plasticity. *J. Mech. Phys. Solid* 48, 1565–1595.
- Acharya, A., Beaudoin, A.J., 2000. Grain-size effect in viscoplastic polycrystals at moderate strains. *J. Mech. Phys. Solids* 48, 2213–2230.
- Aifantis, E.C., 1984. On the microstructural origin of certain inelastic models. *J. Eng. Mater. Tech.* 106, 326–330.
- Aifantis, E.C., 1987. The physics of plastic deformation. *Int. J. Plasticity* 3, 211–247.
- Aifantis, E.C., 1999. Strain gradient interpretation of size effects. *Int. J. Fract.* 95, 299–314.
- Aifantis, K.E., Willis, J.R., 2005. The role of interfaces in enhancing the yield strength of composites and polycrystals. *J. Mech. Phys. Solid* 53, 1047–1070.
- Arsenlis, A., Parks, D.M., 1999. Crystallographic aspects of geometrically-necessary and statistically-stored dislocation density. *Acta Mater.* 47, 1597–1611.
- Arsenlis, A., Parks, D.M., Becker, R., Bulatov, V.V., 2004. On the evolution of crystallographic dislocation density in non-homogeneously deforming crystals. *J. Mech. Phys. Solids* 52, 1213–1246.
- Ashby, M.F., 1970. The deformation of plastically non-homogenous alloys. *Philos. Mag.* 21, 399–424.
- Bazant, Z.P., Pijaudier-Cobot, G., 1988. Nonlocal continuum damage, localization instability and convergence. *J. Appl. Mech.* 55, 287–293.
- Bazant, Z.P., Guo, Z., 2002. Size effect and asymptotic matching approximations in strain-gradient theories of micro-scale plasticity. *Int. J. Solid Struct.* 39, 5633–5657.
- Bassani, J.L., 2001. Incompatibility and a simple gradient theory of plasticity. *J. Mech. Phys. Solid* 49, 1983–1996.
- Bammann, D.J., Aifantis, E.C., 1982. On a proposal for a continuum with microstructure. *Acta Mech.* 45, 91–121.
- Bammann, D.J., 2001. A model of crystal plasticity containing a natural length scale. *Mater. Sci. Eng. A* 309–310, 406–410.
- Begley, M.R., Hutchinson, J.W., 1998. The mechanics of size-dependent indentation. *J. Mech. Phys. Solid* 46, 2049–2068.
- Beaudoin, A.J., Acharya, A., 2001. A model for rate-dependent flow of metal polycrystals based on the slip plane lattice incompatibility. *Mater. Sci. Eng. A* 309–310, 411–415.
- Bergstrom, Y., Hallen, H., 1982. An improved dislocation model for the stress–strain behavior of polycrystalline alpha-iron. *Mater. Sci. Eng.* 56, 47–61.
- Chen, S.H., Wang, T.C., 2002. Interface crack problem with strain gradient effects. *Int. J. Fract.* 117, 25–37.
- Cosserat, E., Cosserat, F., 1909. *Theorie des corp deformables*. Herman, Paris.
- de Borst, R., Mühlhaus, H.-B., 1992. Gradient-dependent plasticity formulation and algorithmic aspects. *Int. J. Numer. Meth. Eng.* 35, 521–539.
- de Borst, R., Sluys, L.J., Mühlhaus, H.-B., Pamin, J., 1993. Fundamental issues in finite element analysis of localization of deformation. *Eng. Comput.* 10, 99–121.
- de Borst, R., Pamin, J., 1996. Some novel developments in finite element procedures for gradient-dependent plasticity. *Int. J. Numer. Meth. Eng.* 39, 2477–2505.
- DeGuzman, M.S., Neubauer, G., Flinn, P., Nix, W.D., 1993. The role of indentation depth on the measured hardness of materials. *Mater. Res. Symp. Proc.* 308, 613–618.
- Elmustafa, A.A., Stone, D.S., 2002. Indentation size effect in polycrystalline F.C.C metals. *Acta Mater.* 50, 3641–3650.
- Eringen, A.C., 1968. Theory of micropolar elasticity. In: Liebowitz, H. (Ed.), *Fracture, An Advanced Treatise*, vol. 2. Academic Press, New York, pp. 621–729.
- Eringen, A.C., Edelen, D.G.B., 1972. On non-local elasticity. *Int. J. Eng. Sci.* 10, 233–248.
- Estrin, Y., Mecking, H., 1984. A unified phenomenological description of work-hardening and creep based on one-parameter models. *Acta Metall.* 32, 57–70.

- Evers, L.P., Brekelmans, W.A.M., Geers, M.G.D., 2004. Scale dependent crystal plasticity framework with dislocation density and grain boundary effects. *Int. J. Solid Struct.* 41, 5209–5230.
- Fleck, N.A., Hutchinson, J.W., 1993. A phenomenological theory for strain gradient effects in plasticity. *J. Mech. Phys. Solids* 41, 1825–1857.
- Fleck, N.A., Muller, G.M., Ashby, M.F., Hutchinson, J.W., 1994. Strain gradient plasticity: theory and experiment. *Acta Metall. Mater.* 42, 475–487.
- Fleck, N.A., Hutchinson, J.W., 1997. Strain gradient plasticity. *Adv. Appl. Mech.* 33, 295–361.
- Fleck, N.A., Hutchinson, J.W., 2001. A reformulation of strain gradient plasticity. *J. Mech. Phys. Solids* 49, 2245–2271.
- Fremond, M., Nedjar, B., 1996. Damage, gradient of damage and principle of virtual power. *Int. J. Solid Struct.* 33 (8), 1083–1103.
- Gao, H., Huang, Y., Nix, W.D., Hutchinson, J.W., 1999a. Mechanism-based strain gradient plasticity – I. Theory. *J. Mech. Phys. Solid* 47, 1239–1263.
- Gao, H., Huang, Y., Nix, W.D., 1999b. Modeling plasticity at the micrometer scale. *Naturwissenschaften* 86, 507–515.
- Gao, H., Huang, Y., 2001. Taylor-based nonlocal theory of plasticity. *Int. J. Solid Struct.* 38, 2615–2637.
- Gracio, J.J., 1994. The double effect of grain size on the work-hardening behavior of polycrystalline copper. *Scripta Metall. Mater.* 31, 487–489.
- Guo, Y., Huang, Y., Gao, H., Zhuang, Z., Hwang, K.C., 2001. Taylor-based nonlocal theory of plasticity: numerical studies of the micro-indentation experiments and crack tip fields. *Int. J. Solid Struct.* 38, 7447–7460.
- Gurtin, M.E., 2002. A gradient theory of single-crystal viscoplasticity that accounts for geometrically necessary dislocations. *J. Mech. Phys. Solid* 50 (1), 5–32.
- Gurtin, M.E., 2003. On a framework for small-deformation viscoplasticity: free energy, microforces, strain gradients. *Int. J. Plasticity* 19, 47–90.
- Haque, M.A., Saif, M.T.A., 2003. Strain gradient effect in nanoscale thin films. *Acta Mater.* 51, 3053–3061.
- Hirsch, P.B., 1975. In: Hirsch, P.B. (Ed.), *The Physics of Metals*, vol. 2. Cambridge University Press, Cambridge, p. 232.
- Hill, R., 1950. *Mathematical Theory of Plasticity*. Oxford University Press, Oxford.
- Hutchinson, J.W., 2000. Plasticity at the micron scale. *Int. J. Solid Struct.* 37, 225–238.
- Huang, Y., Gao, H., Nix, W.D., Hutchinson, J.W., 2000a. Mechanism-based strain gradient plasticity – II analysis. *J. Mech. Phys. Solid* 48, 99–128.
- Huang, Y., Qu, S., Hwang, K.C., Li, M., Gao, H., 2004. A conventional theory of mechanism-based strain gradient plasticity. *Int. J. Plast.* 20, 753–782.
- Huber, N., Nix, W.D., Gao, H., 2002. Identification of elastic–plastic material parameters from pyramidal indentation of thin films. *Proc. Roy. Soc. Lond. Ser. A* 458 (2023), 1593–1620.
- Hwang, K.C., Jiang, H., Huang, Y., Gao, H., Hu, N., 2002. A finite deformation theory of strain gradient plasticity. *J. Mech. Phys. Solid* 50, 81–99.
- Hwang, K.C., Jiang, H., Huang, Y., Gao, H., 2003. Finite deformation analysis of mechanism-based strain gradient plasticity: torsion and crack tip field. *Int. J. Plasticity* 19, 235–251.
- Kiser, M.T., Zok, F.W., Wilkinson, D.S., 1996. Plastic flow and fracture of a particulate metal matrix composite. *Acta Mater.* 44, 3465–3476.
- Konstantinidis, A.A., Aifantis, E.C., 2002. Recent developments in gradient plasticity – Part II: plastic heterogeneity and wavelets. *ASME J. Eng. Mater. Tech.* 124, 358–364.
- Kocks, U.F., 1966. A statistical theory of flow stress and work hardening. *Phil. Mag.* 13, 541.
- Kocks, U.F., 1976. Laws for work-hardening and low-temperature creep. *ASME J. Eng. Mater. Tech.* 98, 76–85.
- Kubin, L.P., Estrin, Y., 1990. Evolution for dislocation densities and the critical conditions for the portevin-lechatelier effect. *Acta Metall. Mater.* 38, 697–708.
- Lasry, D., Belytschko, T., 1988. Localization limiters in transient problems. *Int. J. Solid Struct.* 24, 581–597.

- Lim, Y.Y., Chaudhri, Y.Y., 1999. The effect of the indenter load on the nanohardness of ductile metals: an experimental study of polycrystalline work-hardened and annealed oxygen-free copper. *Philos. Mag. A* 79 (12), 2979–3000.
- Lloyd, D.J., 1994. Particle reinforced aluminum and magnesium matrix composites. *Int. Mater. Rev.* 39, 1–23.
- Ma, Q., Clarke, D.R., 1995. Size dependent hardness in silver single crystals. *J. Mater. Res.* 10, 853–863.
- McElhane, K.W., Valssak, J.J., Nix, W.D., 1998. Determination of indenter tip geometry and indentation contact area for depth sensing indentation experiments. *J. Mater. Res.* 13, 1300–1306.
- Mindlin, R.D., 1964. Micro-structure in linear elasticity. *Arch. Ration. Mech. Anal.* 16, 51–78.
- Mughrabi, H., 2001. On the role of strain gradients and long-range internal stresses in the composite model of crystal plasticity. *Mater. Sci. Eng. A* 317, 171–180.
- Mühlhaus, H.B., Aifantis, E.C., 1991. A variational principle for gradient principle. *Int. J. Solid Struct.* 28, 845–857.
- Nan, C.-W., Clarke, D.R., 1996. The influence of particle size and particle fracture on the elastic/plastic deformation of metal matrix composites. *Acta Mater.* 44, 3801–3811.
- Needleman, A., 1988. Material rate dependent and mesh sensitivity in localization problems. *Comp. Meth. Appl. Mech. Eng.* 67, 68–85.
- Nix, W.D., Gao, H., 1998. Indentation size effects in crystalline materials: a law for strain gradient plasticity. *J. Mech. Phys. Solids* 46, 411–425.
- Pamin, J., 1994. Graded-dependent Plasticity in Numerical Simulation of Localization Phenomena. Dissertation, Delft University of Technology.
- Perzyna, P., 1963. The constitutive equations for rate-sensitive materials. *Quart. Appl. Math.* 20, 321–332.
- Pijaudier-Cabot, T.G.P., Bazant, Z.P., 1987. Nonlocal damage theory. *ASCE J. Eng. Mech.* 113, 1512–1533.
- Poole, W.J., Ashby, M.F., Fleck, N.A., 1996. Micro-hardness of annealed and work-hardened copper polycrystals. *Scripta Mater.* 34, 559–564.
- Qiu, X., Huang, Y., Nix, W.D., Hwang, K.C., Gao, H., 2001. Effect of intrinsic lattice resistance in strain gradient plasticity. *Acta Mater.* 49, 3949–3958.
- Qiu, X., Huang, Y., Wei, Y., Gao, H., Hwang, K.C., 2003. The flow theory of mechanism-based strain gradient plasticity. *Mech. Mater.* 35, 245–258.
- Rhee, M., Hirth, J.P., Zbib, H.M., 1994. A superdislocation model for the strengthening of metal matrix composites and the initiation and propagation of shear bands. *Acta Metall. Mater.* 42, 2645–2655.
- Shrotriya, P., Allameh, S.M., Lou, J., Buchheit, T., Soboyejo, W.O., 2003. On the measurement of the plasticity length scale parameter in LIGA nickel foils. *Mech. Mater.* 35, 233–243.
- Shu, J.Y., Fleck, N.A., 1998. The prediction of a size effect in micro-indentation. *Int. J. Solid Struct.* 35, 1363–1383.
- Sluys, L.J., Estrin, Y., 2000. The analysis of shear banding with a dislocation based gradient plasticity model. *Int. J. Solid Struct.* 37, 7127–7142.
- Stolken, J.S., Evans, A.G., 1998. A microbend test method for measuring the plasticity length-scale. *Acta Mater.* 46, 5109–5115.
- Stelmashenko, N.A., Walls, M.G., Brown, L.M., Milman, Y.V., 1993. Microindentation on W and Mo oriented single crystals: an STM study. *Acta Metall. Mater.* 41, 2855–2865.
- Svensen, B., 2002. Continuum thermodynamic models for crystal plasticity including the effects of geometrically-necessary dislocations. *J. Mech. Phys. Solid* 50, 1297–1329.
- Swadener, J.G., George, E.P., Pharr, G.M., 2002. The correlation of the indentation size effect measured with indenters of various shapes. *J. Mech. Phys. Solid* 50, 681–694.
- Taylor, G.I., 1938. Plastic strain in metals. *J. Inst. Met.* 62, 307–324.
- Taylor, M.B., Zbib, H.M., Khaleel, M.A., 2002. Damage and size effect during superplastic deformation. *Int. J. Plasticity* 18, 415–442.
- Tsagrakis, I., Aifantis, E.C., 2002. Recent developments in gradient plasticity – Part I: formulation and size effects. *ASME Trans. J. Eng. Mater. Tech.* 124, 352–357.
- Valanis, K.C., 1996. A gradient theory of internal variables. *Acta Mech.* 116, 1–14.

- Voyiadjis, G.Z., Deliktas, B., Aifantis, E.C., 2001. Multiscale analysis of multiple damage mechanisms coupled with inelastic behavior of composite materials. *J. Eng. Mech., ASCE* 127, 636–645.
- Voyiadjis, G.Z., Abu Al-Rub, R.K., Palazotto, A.N., 2003. Non-local coupling of viscoplasticity and anisotropic viscodamage for impact problems using the gradient theory. *Arch. Mech.* 55, 39–89.
- Voyiadjis, G.Z., Abu Al-Rub, R.K., Palazotto, A.N., 2004. Thermodynamic formulations for non-local coupling of viscoplasticity and anisotropic viscodamage for dynamic localization problems using gradient theory. *Int. J. Plasticity* 20, 981–1038.
- Voyiadjis, G.Z., Abu Al-Rub, R.K., 2004. Length scales in gradient plasticity. In: Ahzi, S., Cherkaoui, M., Khaleel, Zbib, H.M., Zikry, M.A., LaMatina, B. (Eds.), *Proceedings of the IUTAM Symposium October 2002 on Multiscale Modeling and Characterization of Elastic–Inelastic Behavior of Engineering Materials*. Kluwer Academic Publishers, Morocco, pp. 167–174.
- Voyiadjis, G.Z., Abu Al-Rub, R.K., 2005. Gradient plasticity theory with a variable length scale parameter. *Int. J. Solid Struct.* 42, 3998–4029.
- Voyiadjis, G.Z., Abu Al-Rub, R.K., in press. A finite strain plastic-damage model for high velocity impacts using combined viscosity and gradient localization limiters, Part II: Numerical aspects and simulations. *Int. J. Damage Mech.*
- Wang, W.M., Askes, H., Sluys, L.J., 1998. Gradient viscoplastic modeling of material instabilities in metals. *Met. Mater. Korea* 4 (3), 537–542.
- Yuan, H., Chen, J., 2001. Identification of the intrinsic material length in gradient plasticity theory from micro-indentation tests. *Int. J. Solid Struct.* 38, 8171–8187.
- Zaiser, M., Aifantis, E.C., 2003. Geometrically necessary dislocations and strain gradient plasticity – a dislocation dynamics point of view. *Scripta Mater.* 48, 133–139.
- Zbib, H.M., Aifantis, E.C., 1988. On the localization and postlocalization behavior of plastic deformation, I, II, III. *Res. Mech.* 23, 261–277, 279–292, 293–305.
- Zbib, H.M., Rhee, M., Hirth, J.P., 1998. On plastic deformation and the dynamics of 3D dislocations. *Int. J. Mech. Sci.* 40, 113–127.
- Zbib, H.M., Aifantis, E.C., 2003. Size effects and length scales in gradient plasticity and dislocation dynamics. *Scripta Mater.* 48, 155–160.
- Zhu, H.T., Zbib, H.M., 1995. Flow strength and size effect of an Al–Si–Mg composite model system under multiaxial loading. *Scripta Metall. Mater.* 32, 1895–1902.